

AUTOMATING FOREST STAND DELINEATION USING AERIAL IMAGERY AND LiDAR

by

ADVAIT SANKHE

(Under the Direction of Frederick Maier)

ABSTRACT

Forest stands are fundamental management units, consisting of trees of uniform composition and structure. Creating stand maps is subjective, time-consuming and requires expertise. The dynamic nature of forests necessitates regular updates and revisions to stand maps. This thesis aims to provide automated methods of tackling this problem, using both aerial imagery and LiDAR. We first examine the effectiveness of traditionally employed metrics to evaluate stand maps over three forested landscapes of varying complexity and degrees of management. We present a fast workflow within ArcGIS Pro that is aimed at maximizing homogeneity of stands while allowing flexibility in terms of the feasibility of stand sizes. To address the issue of subjectivity between experts and the requirements of the land, we also propose an alternative, hands-on approach for refinement using random forests. This significantly reduces human effort while maintaining the required precision.

INDEX WORDS: Forestry, Remote Sensing, Geographic Object-based Image Analysis, Image Segmentation, Random Forests, Stand Delineation, LiDAR, ArcGIS Pro.

AUTOMATING FOREST STAND DELINEATION USING AERIAL IMAGERY AND LiDAR

by

ADVAIT SANKHE

Bachelor of Technology, Mumbai University, 2022

A Thesis Submitted to the Graduate Faculty of the
University of Georgia in Partial Fulfillment of the Requirements for the Degree.

MASTER OF SCIENCE

ATHENS, GEORGIA

2025

©2025

Advait Sankhe

All Rights Reserved

AUTOMATING FOREST STAND DELINEATION USING AERIAL IMAGERY AND LiDAR

by

ADVAIT SANKHE

Major Professor: Frederick Maier

Committee: Khaled Rasheed

Can Vatandaslar

Electronic Version Approved:

Ron Walcott

Dean of the Graduate School

The University of Georgia

August 2025

ACKNOWLEDGMENTS

I am deeply grateful to my advisor, Dr. Frederick Maier, for his constant guidance and support throughout this project, and for going above and beyond to ensure that things were on track and proceeding smoothly. I would like to extend my sincere appreciation to Dr. Can Vatandaslar for his invaluable insights in forest management practices and to Dr. Khaled Rasheed for his help in the technical aspects of data analysis. Special thanks to Bahaa for his contributions in the form of constructive critiques and ideas that helped improve this project. I am also thankful to the larger AI and PERSEUS teams for giving me the opportunity to explore the intersection of AI and forestry, as well as for the platform to present and discuss my work on multiple occasions. Finally, I wish to acknowledge everyone that kept me company in the student office throughout this journey. Thank you.

This work is supported by USDA NIFA #2023-68012-38992, Promoting Economic Resilience and Sustainability of the Eastern U.S. Forests (PERSEUS), with assistance from the UGA Warnell School of Forestry and the UGA Institute of Artificial Intelligence.

CONTENTS

| | |
|---|------------|
| Acknowledgments | iv |
| List of Figures | vii |
| List of Tables | ix |
| 1 Introduction | 1 |
| 1.1 Background and Motivation | 1 |
| 1.2 Contributions | 2 |
| 2 Background and Related Literature | 6 |
| 2.1 Remote Sensing and Forestry | 6 |
| 2.2 Segmentation and Decision-Making Techniques | 8 |
| 2.3 Stand Delineation | 12 |
| 3 Study Areas and Datasets | 18 |
| 3.1 Study Areas | 18 |
| 3.2 Remote Sensing Sources and Data Processing | 20 |

| | | |
|----------|---|-----------|
| 4 | Automated Stand Delineation – Homogeneity-based approach | 25 |
| 4.1 | Evaluation Metrics | 26 |
| 4.2 | Methodology | 31 |
| 4.3 | Results and Discussion | 35 |
| 5 | Human-involved Approach | 47 |
| 5.1 | Methodology | 48 |
| 5.2 | Results and Discussion | 52 |
| 6 | Conclusion | 60 |
| | Bibliography | 63 |

LIST OF FIGURES

| | | |
|-----|---|----|
| 1.1 | Example of a forest stand map. | 3 |
| 2.1 | Intuitive way of understanding the Mean Shift Procedure. Image Source: [2] | 10 |
| 2.2 | Example of decision tree. | 11 |
| 3.1 | Study Area: Talladega National Forest | 19 |
| 3.2 | Reference stand map for the privately owned property on the outskirts of the Talladega National Forest. | 23 |
| 3.3 | Reference stand map for the Whitehall Forest. | 24 |
| 4.1 | Cases of overlaps and reflected $RA_{or}\%$ and $RA_{os}\%$ values. A better segmentation would yield higher and more equal $RA_{or}\%$ and $RA_{os}\%$ values. Numbers in colored regions indicate area (units unspecified). | 39 |
| 4.2 | Oversegmentation ($IoU = 0.09$, $RA_{or}\% = 21.8$, $RA_{os}\% = 52.9$) | 40 |
| 4.3 | Good Segmentation ($IoU = 0.39$, $RA_{or}\% = 42.4$, $RA_{os}\% = 43.1$) | 40 |
| 4.4 | Undersegmentation ($IoU = 0.22$, $RA_{or}\% = 58.3$, $RA_{os}\% = 24.8$) | 40 |
| 4.5 | Visualizing the effects of supervised metrics. | 40 |
| 4.6 | Examples of segmentations and respective values of unsupervised metrics. | 41 |

| | | |
|------|---|----|
| 4.7 | Example of derived Riparian zones | 42 |
| 4.8 | Overview of delineation methodology using ArcGIS Pro | 42 |
| 4.9 | Degree of variance of a property explained by segmentation (R^2). | 43 |
| 4.10 | Delineations created using our algorithm over CHM rasters. | 44 |
| 4.11 | CHM based delineations, overlaid on volume maps as discussed in 4.10. | 45 |
| 4.12 | Whitehall map derived from our methodology (left) and derived map after masking roads (right), compared to reference map (center), as presented in Table 4.3. | 45 |
| 4.13 | Segmentation created by initially masking derived riparian zones. | 46 |
| 5.1 | Human-involved delineation - Step 1: Generate microstands | 49 |
| 5.2 | Human-involved delineation - Step 2: Create samples | 50 |
| 5.3 | Human-involved delineation - Step 3: Random Forest Merging + Smoothing | 52 |
| 5.4 | Nearly 450 stands created by the expert by merging microstands. Microstands merged over different ‘compartments’ within the study area. | 54 |
| 5.5 | Nearly 310 stands created by the expert by merging microstands. Microstands merged over neighboring compartments within the study area. | 56 |
| 5.6 | Generated Whitehall Map, showing selected areas | 58 |
| 5.7 | Reference Whitehall Map, roads masked out | 58 |
| 5.8 | Whitehall map derived by the human-involved approach, as presented in 5.5 | 58 |
| 5.9 | Talladega: High confidence threshold stands (left). Oversegmented, requiring post- processing or reiteration of the human-involved method. Requires effort but simpler to fix. (Right) Low confidence threshold. Undersegmented, difficult to fix once generated. | 59 |

LIST OF TABLES

| | | |
|-----|--|----|
| 3.1 | Details of reference stand maps | 23 |
| 4.1 | Comparing Reference Maps | 35 |
| 4.2 | Values of unsupervised metrics of stand maps created by experts. | 36 |
| 4.3 | Comparing results over Whitehall. | 37 |
| 4.4 | Obtained results after masking riparian zones. Outputs visualized in Figure 4.13 | 38 |
| 5.1 | Comparing microstand and reference maps for the larger Talladega area | 53 |
| 5.2 | Evaluation metrics for stands created by the human-involved approach: disjoint com- partments. | 55 |
| 5.3 | Evaluation metrics for stands created by the human-involved approach: connected com- partments. | 57 |
| 5.4 | Evaluation metrics for stands created by the human-involved approach: compartment 60. . . . | 57 |
| 5.5 | Evaluation metrics for stands created by the human-involved approach: Whitehall. . . . | 58 |

CHAPTER I

INTRODUCTION

I.1 Background and Motivation

Stands are a fundamental management unit in forest management and planning. They are typically a community of trees having a uniformity in species composition and structure (height, diameter at breast height, etc.) that distinguishes them from neighboring communities. A forest can thus be seen as a mosaic of forest stands. This is illustrated in Figure 1.1.

Management decisions are typically applied over forest stands instead of individual trees. The main idea behind delineating stands is to improve management efficiency over large forest areas. Management actions such as clearcutting, thinning, and prescribed burning are generally performed over entire stands. Stands are also used to keep track of inventory, plan activities, and calculate revenue. It is thus important to have accurate, up-to-date stand maps.

Forests cover large areas and can exhibit incredibly complex, non-homogeneous landscapes. They are also dynamic ecosystems, where natural disturbances such as wildfires and harvesting can drastically alter their structure. This in turn necessitates frequent updates and revisions of stand maps.

Traditionally, experts have performed stand delineation through visual inspection of aerial or satellite imagery. The process of creating well-defined stand maps requires domain expertise, an implicit understanding and knowledge of forest management practices and constraints. Stands are delineated according to the expert's opinions on their utility. There is no established 'ground-truth' stand map. Thus, there is a good deal of subjectivity associated with the creation of stand maps.

This thesis explores methods of automating stand delineation in an objective manner. The main motivation behind automating this process is to drastically reduce the time and effort needed to create, update and revise stand maps. This thesis also highlights the challenges that both an algorithm and a human may face when delineating stands over complex forest landscapes [23].

1.2 Contributions

Chapter 2 of this thesis provides a brief overview of the problem and presents relevant concepts in remote sensing and AI. Important concepts relating to Light Detection and Ranging (LiDAR), aerial imagery, and the derivation of vegetation indices, canopy heights, and ground elevation are discussed. There is a further discussion on mean shift segmentation/clustering algorithms along with an explanation on random forest models. Next, an overview of research on automated stand delineation performed over the last two decades is provided. In our view, there has been relatively limited work in this field. A common issue with the existing literature is the inconsistencies with the types of data used and the variety of evaluation techniques.

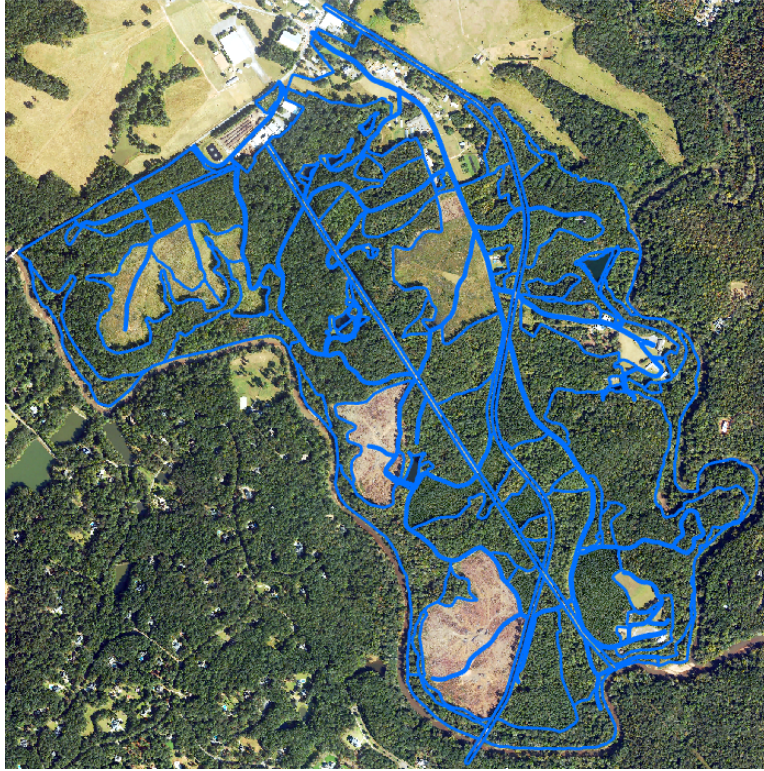


Figure 1.1: Example of a forest stand map. Every polygon represents an individual stand that is uniform and distinct from its neighbors. The forest is thus a ‘mosaic’ of stands.

Many studies are based on small, well-managed research forests, where the scope of the problem is much more limited than in practical use cases. There is also some discussion in the literature [23][26], regarding the validity of the stand concept, and perhaps having much smaller, algorithmically derived management units should be preferred.

Chapter 3 introduces the study area and materials that used in this thesis. The study areas consist of 1) the Talladega National Forest, a large, highly spatially complex region with uneven topography and mixed-species stands; 2) a privately-owned managed area located on the outskirts of Talladega; and 3) the Whitehall Forest, a well-managed research forest a few miles south of the University of Georgia’s primary campus in Athens, Georgia.

There are two main data sources used in our study. The first is the aerial imagery (RGB + the near-infrared (NIR) band) obtained by the Natural Agricultural Imagery Program (NAIP [1]) and airborne LiDAR data over the Talladega forest and outskirts. Terrestrial LiDAR was used in the Whitehall area. The other important resource is the set of independent, expert created stand maps across the study areas. The stand maps are highly detailed, separating timber types and having allocated stands for steep areas. The stand maps distinguish between species of pine (e.g. longleaf pines versus loblolly pines), upland versus bottomland hardwoods and more. The Talladega National Forest stand map contains mixed-species stands which are labeled accordingly. There is a high variability in the sizes of stands in all study areas. There is also a difference in how polygons are used in the different stand delineation maps. For example, the stand maps created for the Talladega National Forest depict roads as separating lines between stands, whereas roads in the Whitehall Forests are polygons themselves.

We start Chapter 4 by introducing the evaluation metrics used for judging the quality of stand maps. In general, these fall into two broad categories, supervised metrics and unsupervised metrics. The characteristics of the supervised and unsupervised metrics are explained in detail with visual examples. A comparison between two independently created reference maps over the same area highlights the subjectivity in delineation, as reflected by the moderate values of the supervised metrics. We also analyze the complexity of the reference maps with respect to stock variables such as tree volume and biophysical characteristics such as the Canopy Height Model (CHM) and Normalized Difference Vegetation Index (NDVI). The explained variance in the variables by the delineations illustrates the difficulty in delineation of various landscapes. It is to be noted that the metrics show that none of the reference stand maps are particularly focused on maximizing the homogeneity of stock variables.

We then present a workflow within ArcGIS Pro to quickly generate stand maps over three or single band rasters which prioritizes homogeneity of a given property. The workflow is relatively flexible in terms of managing the homogeneity versus size of stands. We present our results over the three study areas and discuss their qualities. We also provide a method of masking out riparian zones. These are very prevalent in the Talladega National Forest and are hard for segmentation algorithms to work with.

Through our experiments and the existing literature, it is very clear that the task of stand delineation is hard to treat completely objectively. For this reason, Chapter 5 introduces an alternative method of approaching the problem, one which requires greater involvement from the end user. In this approach, an initial microstand map is generated which provides the end user with a guideline for creating a collection of stands. This reduces the effort needed to draw precise polygons. The stands that the user creates then serve as training samples for a Random Forest model to learn how to form *real* stands from the microstand map. Chapter 5 presents the results of this methodology, with different strategies for creating stand maps and different hyperparameters for the classification model. We also compare our results with the results obtained in the previous chapter. The model needs to be improved upon in order to generalize well across the forest landscape. However, the microstands that ease the creation of stands perform well in comparison to creating stands on a blank canvas. By iteratively and appropriately using the microstand merging and random forest merging steps, the process of stand delineation can be improved and made easier.

CHAPTER 2

BACKGROUND AND RELATED LITERATURE

The process of large-scale automated stand delineation requires detailed remote sensing data and the utilization of AI techniques involving approximation, optimization and segmentation. The following sections provide relevant conceptual background and discuss the existing research literature on this problem.

2.1 Remote Sensing and Forestry

Remote sensing plays a significant role in modern forestry practices. Large-scale imagery allows highly precise details to be used in resource assessment, monitoring and analysis. Hyperspectral images can be used to calculate vegetation indices, image transformations that highlight certain vegetation properties such as photosynthetic activity. One of the most commonly used indices, which has been employed in

this thesis, is the Normalized Difference Vegetation Index (NDVI), which can be used to assess vegetation health and density.

LiDAR is a remote sensing method of determining distances of objects, based on the time taken for the LiDAR device to receive reflected light rays transmitted by a laser on the device. For example, a ray of light transmitted by an aerial LiDAR device will take longer to hit the ground than it will to hit the crown of a tree. LiDAR samples an area, making multiple point-wise measurements. The result is a three dimensional (3D) “point cloud map” of a tree or entire forest.

The LiDAR point cloud can be used to calculate several zonal statistics over an area. For example, we can calculate the percentage of points above 2m in a 30m by 30m area. A 2D raster map with a ground resolution of 30m can then be created, with every pixel representing the value of this statistic. The percentage of points above 2m (pzabove2) statistic is useful for estimating canopy density, as it separates ground, grass and shrubbery points from the points representing a tree. The “lidR” [20] package in the R programming language contains preprocessing tools to derive such LiDAR metrics in the form of 2D raster maps. Examples of metrics include the maximum height (zmax), minimum height (zmin), mean intensity (imean) and many others.

These metrics can then be used to create models of the landscape. Using the lowest points of the point cloud, we can create a representation of the surface elevation of the earth, called the Digital Elevation Model (DEM). The Digital Surface Model (DSM) on the other hand, represents the highest points of the point cloud (assuming no noisy points in the data). In the example of forests, we can then naturally conclude that the height difference between the DSM and the DEM would then represent the height of a canopy. This is called the Canopy Height Model (CHM). Other metrics such as the slope of the terrain may also be derived from the DEM.

Forest inventory variables are key to analysis and management of forest resources. These include the stock variables diameter at breast height (DBH), basal area, above ground biomass, tree volume, and trees per unit area (e.g., acre). These are useful in estimating the potential of growth and value of a stand in managed forests. Typically, measurements are manually made by forestry professionals over forest sample plots. Lee et al. [25] discuss ways of estimating and mapping these metrics over larger areas. They use field measurement data from 255 plots over the Talladega National Forest. Using regression models, an estimation of the stock variables can be created as a combination of several LiDAR metrics. These models can then be used to impute the volume, basal area and above ground biomass over the entire forest.

2.2 Segmentation and Decision-Making Techniques

2.2.1 Mean Shift Segmentation

One of the primary segmentation techniques that was employed in this study is Mean Shift Segmentation, as implemented in the ArcGIS Pro tool. Mean shift, in the context of clustering, can be considered as an iterative approach to finding the local maxima of a density function in a feature space (Fig 2.1). The feature space typically consists of instances defined by the (x,y) spatial coordinates and the raster pixel values (1 band or 3 bands in most cases).

First, a window is defined around every instance based on the bandwidth parameters of a kernel function. The kernel function is used to calculate the density of the feature space. Kernel functions can be binary, as shown in Eq. 2.1, where λ is the bandwidth, i.e., the window around which all the points are equally weighted.

$$K(x) = \begin{cases} 1 & \text{if } \|x\| \leq \lambda \\ 0 & \text{otherwise} \end{cases} \quad (2.1)$$

A gaussian kernel function is also commonly used, where closer points are given higher weights (Eq. 2.2). The gaussian kernel is a smoother function that ensures less abrupt breaks in the segmentation.

$$K(x) = e^{-\frac{\|x\|^2}{2h^2}} \quad (2.2)$$

Here, h is the bandwidth parameter, which is commonly set to the standard deviation of instances in the feature space.

For every instance, the kernel function is used to calculate the weighted mean of the pixels/instances within the window. The instance is then *shifted* to this new mean/center of gravity. This is the mean shift procedure and the direction and magnitude by which the instance is shifted is called the mean shift vector. This procedure occurs simultaneously for every instance in the feature space. This process goes on iteratively until convergence, i.e., the search window does not shift as it has reached a mode. Every window/instance that ends up near the same mode is merged to form a cluster [3][6].

Although the inner workings of the Mean Shift Segmentation Tool in ArcGIS Pro are not published, it is assumed that it follows a similar procedure to segment rasters, taking the (x,y) coordinates and raster pixel values into account. Typical hyperparameters in mean shift segmentation are the spectral importance (pixel values), spatial importance (proximity of pixels) and a minimum cluster size (merge small nearby clusters until they reach a minimum size).

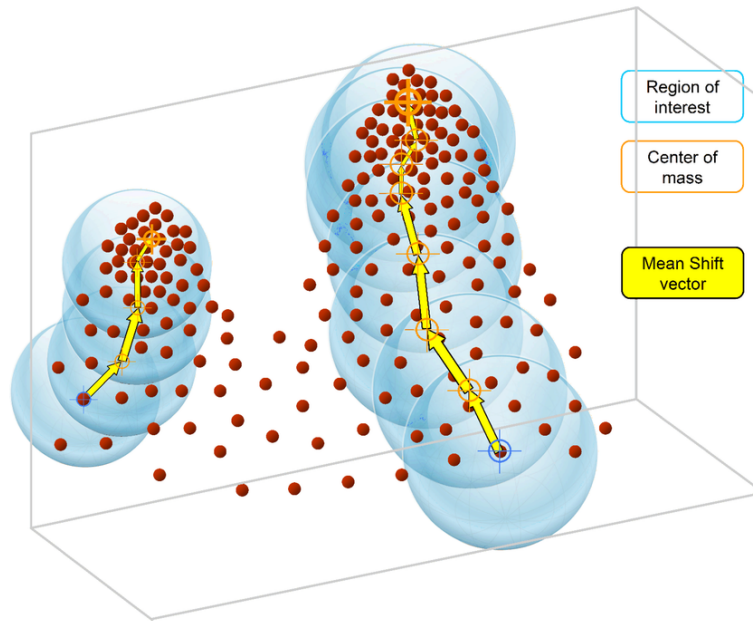


Figure 2.1: Intuitive way of understanding the Mean Shift Procedure. Image Source: [2]

2.2.2 Random Forest Classifiers

Random Forest [9] is a commonly used ensemble machine learning technique, based on training an ensemble (collection) of independent decision trees that collectively vote on predicting a value during inference. A decision tree is a machine learning model typically used for classification. It is a directed graph consisting of a single root node and one or more leaf nodes. An instance (object) to be classified enters the tree at the root node and based upon its feature values traverses a single branch of the tree. The leaf the instance ultimately enters determines its classification label.

For example, a decision tree for determining whether bank loans should be approved given credit score and income is shown in Figure 2.2. Based on the tree, a loan for an applicant earning \$50,000 and having a credit rating of 800 would be approved.

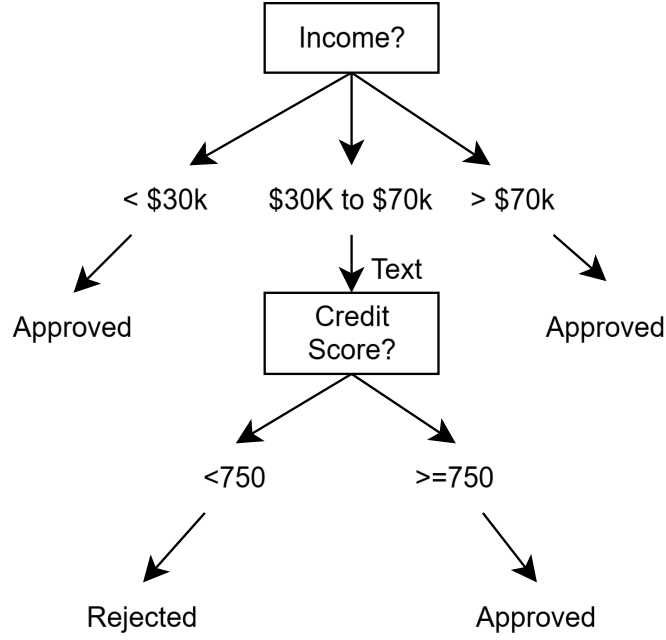


Figure 2.2: Example of decision tree.

Decision trees are typically created using a supervised learning method and a training set of instances. The process is typically iterative and greedy. Starting with the root node, the tree is expanded in an attempt to partition the training set into groups of instances having the same classification label. Formally, desirable groups at the leaves have low entropy or (equivalently) high information gain (IG) relative to their parents. Equations for entropy and IG are shown below.

$$\text{Entropy}(Y) = - \sum_{i=1}^C p_i \log_2(p_i)$$

$$\text{IG}(Y, X) = \text{Entropy}(Y) - \sum_{v \in \text{Values}(X)} \frac{|S_v|}{|S|} \text{Entropy}(S_v)$$

where Y is the variable to be classified into one of the classes in C . p_i represents the proportion of class i in C . S_v represents the subset of feature X where $X=v$ and S is the entire dataset. A high information gain indicates a reduction in entropy. Thus, the feature X which maximizes information gain is chosen to efficiently split the dataset into branches.

Decision trees, while having a quick inference and training time, are sensitive to outliers and can overfit easily. Random Forests help with the overfitting problem of decision trees by creating a ‘forest’ of decision trees that are trained on different samples of the training data. The sampling of training instances is done through the *bagging* process. Bagging or bootstrap aggregating, is a process where a random sample with replacement of the training set is used to fit the decision tree. This is done B times (the number of trees in the random forest). At inference, voting can be binary (‘yes’ or ‘no’) or probabilistically ((number of yes)/(total samples at the leaf node of an individual tree)). Random Forest methods contain hyperparameters such as the number of decision trees used, maximum depth of decision trees and minimum number of samples at leaf node. These hyperparameters help avoid hyper-specific inference rules. We employ the random forest algorithm in our study in human-involved delineation process, where decision trees vote on whether a pair of microstands must be merged to form a ‘real’ forest stand.

2.3 Stand Delineation

Forest stand delineation has been typically approached as geographic object-based image analysis (GEO-BIA)/image segmentation problem. The multiresolution segmentation (MRS) tool in the Trimble eCognition [7], a software for geospatial analysis, has been commonly employed for this task in the existing

literature. The tool allows stacking multiple rasters to be used as the input for segmentation. Allowing the user to adjust the weights for chosen bands (e.g., placing greater importance on CHM over NDVI), along with parameters like the scale, shape and compactness enables a good deal of flexibility. Most of the works in the literature which employed eCognition base their results on trial and error with the multiresolution segmentation parameter settings. Some of the key works that used the eCognition software are described below.

2.3.1 eCognition and Trial & Error based works

Ke et al. [12] tried to determine the ideal parameters and input rasters for the MRS algorithm with respect to the relative overlap metrics (discussed further) to find the ideal scale for segmentation. They performed experiments over multiple sources of data, and observed that a combination of LiDAR and spectral data yielded the best results while also providing the set of layers and hyperparameters used. The latter is not very useful when it comes to generally adapting to the forested areas and requirements in this thesis. A similar study was performed by Ozkan et al. [16] over a mixed forest with the same conclusions.

Sanchez-Lopez et al. [21] provided a semi-automated evaluation strategy to find the best raster and parameters to be used for delineation. The 95th percentile of height and stratum above 30m were found to be the most correlated to stand height and biomass, based on existing literature. Five other rasters were chosen, narrowed down from a set of 36 LiDAR metrics based on correlation analysis. The ideal segmentation for each raster was determined by exhaustively searching through the eCognition parameters. The ‘ideal’ segmentation was based on an unsupervised evaluation method. The global score, a metric that combines weighted variance (measuring intrastand homogeneity) and the Moran’s Index (measuring

interstand heterogeneity) was used for this purpose. It is important to note that the ‘ideal’ segmentation for every input raster can be drastically different.

The next stage of the process involved comparing the ‘ideal’ segmentations of each of these metrics to a ‘ground-truth’, reference stand map. The comparison was done using overlap metrics, taking into account the undersegmentation/oversegmentation of stands. Thus, the optimal raster (95th percentile of height in this case) to be used as the input, based on maximizing homogeneity and likeness to reference stands was found. This study has two main points of criticism. One being that the reference stands only consisted of clearcuts, and so may not be adaptable to stands formed due to other reasons. Secondly, the idea of maximizing homogeneity encourages the creation of overly segmented stand maps with tiny stands. However, forest managers typically do not prefer very small stands due to operational reasons. Thus, there is a need for a post-processing step to remove unnecessary borders in the generated map.

Xiong et al. [8] incorporated tree species maps into their delineation process. The process consisted of generating a superpixel map (a map consisting of microstands) with the CHM and then iteratively merging homogeneous polygons based on certain thresholds like average height, tree proportion, dominant species, etc. These thresholds were determined empirically and there does not seem to be a clear reasoning towards choosing the threshold values. They obtained highly homogeneous polygons and a good overlap with the reference polygons.

However, they also relied on hyperspectral imaging for vegetation indices, which helped create a tree species map. They used a Support Vector Machine (SVM) to classify pixels into one of six classes. The training details of the SVM developed are unclear, although it may be fair to assume that the testing and training area were the same given the highly accurate results of the SVM. Importantly, the study also took

place over a forest farm, exhibiting an easy forest condition. A highly accurate, high resolution tree species map tends to trivialize the problem in a forest farm-like area.

2.3.2 Alternative Methods

The GEOBIA methods provided in eCognition are popular because they are fast and easy to use. Once a delineation is created, an expert can visually assess the results and adjust parameters accordingly. This is then followed by deeper analysis of the obtained stand map. However, there is a lack of control with the process as the delineation is too heavily reliant on the MRS (multiresolution segmentation) algorithm. Alternative methods of delineation are discussed below.

Pukkala et al. [18][17][26] along with Sun et al. [24] moved away from eCognition and tested their own segmentation techniques, including region-growing methods, cellular automata, self-organizing maps and simulated annealing. The data used in their experiments included basal area, mean diameter and LiDAR data for close to 5000 plots with a radius of 25m. Thus, with these data points, they initially narrowed down LiDAR metrics to five which were the most correlated to the stock variables using regression methods. Also, these metrics were then imputed over the entire area using the 3 nearest neighbor method. These metrics were then used as an input for their chosen segmentation algorithm, followed by a smoothing step, done via a mode filter. The results were evaluated based on the degree of variance of the stock variables that was explained by the delineation (R^2). The results obtained favored smaller stands, and the authors believe that having smaller units of management allows for more accurate calculations.

Lepannen et al. [15] compared the results of their CHM-based inputs with eCognition with their iterative region growing algorithms based on 3-band raster consisting of heights, % vegetation and % hardwood volume. These bands were chosen by experts with domain expertise. With their comparisons

to manually delineated stands, they observed that LiDAR was effective and separating stands of different timber size and density, whereas color infrared (CIR) imagery was useful with respect to tree species identification. However, the stands generated were not large enough to be economically feasible. The study area too, was only about a 67 ha commercial forest property.

Dechesne et al. [4] performed studies with respect to object/superpixel creation via quickshift and SLIC (Simple Linear Iterative Clustering) segmentation. Features using high resolution imagery, vegetation indices and LiDAR metrics were calculated for each of these objects. These were then used as training samples for a Random Forest algorithm, where each object was assigned a vegetation class based on the French Forest Landcover Database. Thus, the entire area was then segmented into superpixel objects which were assigned a vegetation class. To convert the superpixel map into a stand map and to deal with noisy objects, experiments using various regularization algorithms was performed to obtain smooth stand polygons.

Other works focused entirely on getting highly accurate superpixel or microstand maps. Caner et al. [5] used a modified SLIC algorithm, the RF-SLIC algorithm where the spectral distance was replaced by the outputs of a random forest regressor. The spectral distance was thus replaced by what the random forest would predict as its ‘distance’ from a different stand class. The microstands were then judged based on boundary accuracy metrics at the pixel level with a small buffer with respect to the reference stands. The boundary precision, specificity and sensitivity showed better outcomes than the microstands created with traditional segmentation algorithms.

The thesis builds upon some of the ideas put forth by the existing literature. As with most other papers, the thesis also evaluates stands with respect to stock variables. Keeping the original purpose of stands, which is to maximize timber management efficiency and revenue in mind, we evaluate stands by

their ability to explain the variance in tree volume. Perhaps more importantly, we examine and expand upon the prevalent idea of evaluating generated stand maps with respect to reference ‘ground truth’ maps, and the issues and challenges that arise by doing so. This leads us to the second, novel approach towards stand delineation that is presented in this thesis. As the evaluation metrics by themselves do not do a very good job at determining the effectiveness of stand maps, we put more control into the hands of the end user as the stand maps are being generated. This methodology takes some ideas regarding microstand creation and merge thresholds from the existing literature, and reimagines them through a user-centric lens.

Recently, Vatandaslar et al. [27] performed stand delineation experiments and analysis using ArcGIS Pro over the Talladega National Forest. Stands were created using the Mean Shift Segmentation and Smooth Polygon tools and visual analysis of the outcomes were presented from a forest management planning perspective. It was noted that the results in this highly heterogeneous and complex area had low to moderate correspondence with the maps created by human practitioners. The work presented in this thesis expands upon this study to create more accurate stand delineation maps while reducing the time required for analysis.

CHAPTER 3

STUDY AREAS AND DATASETS

3.1 Study Areas

The study was performed over three areas of varying degrees of complexity and management. The complexity of an area is influenced by the size, topographic variation, diversity in tree species, and many other characteristics. For instance, a forested area that has a history of being managed with planned activities such as thinning and clearcutting is more likely to contain homogeneous patches of trees of uniform species composition and structure (age, height, etc.).

The first and primary study area for this thesis is the Talladega National Forest. More specifically, we examine the Talladega and Shoal Creek Ranger Districts of the Talladega National Forest, located in the northeastern region of Alabama, USA (fig 3.1). The 93,700 ha area is mainly dominated by natural forests. The forest is characterized by an oak-hickory-pine system, where longleaf (*Pinus palustris*), loblolly (*P. taeda*), shortleaf (*P. echinata*) pines, oaks (*Quercus sp.*), red maple (*Acer rubrum*), hickory (*Carya sp.*), yellow-poplar (*Liriodendron tulipifera L.*) are prevalent tree species. The area has a subtropical

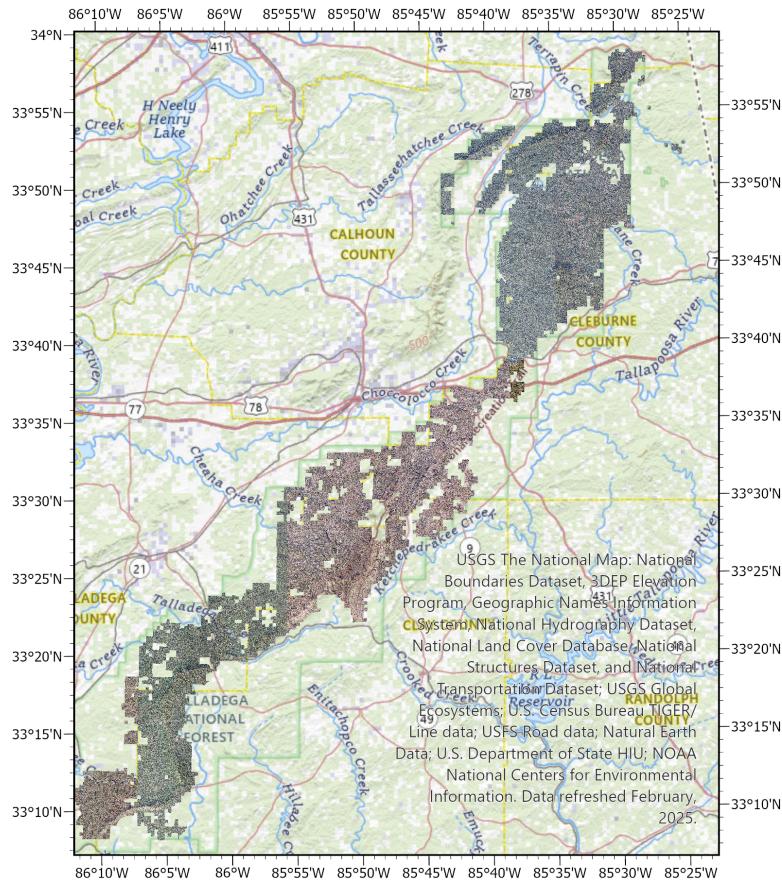


Figure 3.1: Study Area: Talladega National Forest

climate with an average annual precipitation of 1260 mm, and the elevation varies between 152 m and 734 m above sea level [19]. The Talladega National Forest is highly heterogeneous in terms of species and biophysical structure. The forest contains multiple, highly mixed-species stands. The landscape has an uneven topography and has gone through frequently prescribed burns. There have been other natural disturbances, e.g., the Jacksonville Tornado in 2018 damaged nearly 2294 ha of pine cover in the northern part of the landscape. Pine stands are also sensitive to wildfires, with the historical fire return interval reported to be around three years. The frequency of these has decreased due to aggressive fire suppression

efforts over the last century. Therefore, the USDA Forest Service tries to mimic historical fire dynamics by conducting prescribed burns periodically on appropriate sites across Talladega [10].

The second study area is a privately-owned property located adjacent to the Talladega National Forest. It can be thought of as an extension to the landscape of the northern parts of the previous study area, with some similar characteristics. This is a nearly 566 ha area consisting of pines, hardwoods and some fields. Most of the available data and rasters used in the study for the Talladega National Forest extend to this privately-owned area as well.

The third study area is the Whitehall Forest, covering approximately 330 ha in the Piedmont region's Clarke and Oconee Counties. It is approximately 8 km from downtown Athens, Georgia. The forest is managed and utilized by the University of Georgia primarily for research and teaching purposes. It is comprised of natural pine, planted pine, upland hardwood, and bottomland hardwood stands from a broad range of developmental stages. Specifically, shortleaf and longleaf pines dominate the coniferous stands. Oak sp., hickory, red maple, American hornbeam (*Carpinus caroliniana*), yellow-poplar, and sweetgum (*Liquidambar styraciflua*) are common hardwood species in the study area. While the under-story vegetation is absent or minimal, litter cover is typically deep on the forest floor [25][13]. The USDA Soil Survey maps show that the Whitehall Forest is characterized by sandy clay loam, loamy sandy, and alluvial soil types.

3.2 Remote Sensing Sources and Data Processing

We used two remote sensing sources to perform image analysis. The first was the United States Department of Agriculture's (USDA) National Agriculture Imagery Program (NAIP [1]) orthoimages. NAIP provides

publicly available orthoimages (geometrically rectified aerial image rasters) for most parts of the United States, including the Talladega National Forest. These rasters can be downloaded from USDA's Geospatial Data Gateway website as natural color and color infrared mosaics at 0.3 m spatial resolution. Our dataset was collected during the leaf-off season in 2021.

In the next step, we created a NDVI raster using the ArcGIS Pro's raster calculator tool based on the NAIP near-infrared orthomosaic. NDVI is a popular remote sensing index to quantify vegetation greenness and is useful in understanding live vegetation density and assessing changes in plant health. It is calculated as follows:

$$(NIR - R)/(NIR + R) \quad (3.1)$$

With the NIR and R bands both ranging from 0-255 (representing the intensity of the pixel in an 8-bit system). The red band ranges from a wavelength of 650nm to 700 nm whereas the NIR band ranges from 750 to 1400nm. The NDVI value thus ranges from -1 to 1, with higher positive values indicating dense, healthier vegetation and lower positive values meaning less or no lively vegetation. The negative values often indicate water bodies [14].

The second remote sensing source was airborne laser scanning (ALS) data collected by a Leica Terrain Mapper at the topographical quality level 2 during late 2020 and early 2021. While the average density of the LiDAR point cloud was around 5 points per square meter, the horizontal and vertical accuracy of the dataset were 0.71 m and 0.051 m, respectively. LiDAR was unavailable in some areas that were considered to be outside the forest property and/or were privately owned. First, DTM and DSM of the study area were created based on the ground and first LiDAR returns, respectively. Then, the CHM was created by

subtracting DTM from DSM. Finally, several LiDAR metrics were calculated using the *lidR* library in R based on the CHM [20].

We used some layers characterizing the topography of the Talladega National Forest. Thus, the rasters used in the present study can be divided into three classes: optical image layers (e.g., NIR orthomosaic and NDVI), LiDAR-derived layers (e.g., CHM, canopy density, etc.) and topographic layers (e.g., DEM).

We also have two sets of reference stand maps that were created by independent experts. These stand maps contain nearly 6300 stands each, over 250 compartments, covering around 70% of the forest area. The primary stand map that we will be using in this study was developed by researchers at the UGA Warnell School of Forestry and Natural Resources. The average size of a reference stand is 9.7 ha with a standard deviation of 12.1 ha. These stands are smooth and were created by experts through visual inspection of naturally colored orthoimagery. The stands are labeled with the dominant tree species. However, many stands are mixed, i.e., they consist of two or more species. Some of the less homogeneous stands are thus labeled as mixed, with a mention of the two most dominant species. There also exist very large polygons that extend over the entire forest. These are the riparian zones, that are designated areas around the banks of streams that have special management regulations for ecological reasons.

The stand map for the privately owned area on the outskirts of the Talladega National forest was created by a graduate research assistant at the Warnell School of Forestry and Natural Resources. This 566 ha area consists of 41 stands with an average area of 13.3 ha and a standard deviation of 27.5 ha. This stand map was also created through visual inspection of natural color aerial imagery.

The Whitehall forest consists of well defined, homogeneous stands, managed by researchers at the Warnell School of Forestry and Natural Resources, UGA. The stand map also includes non-forest ‘stands’ like the interior roads or the Georgia Power Row. These polygons in turn play a large role in separating the



Figure 3.2: Reference stand map for the privately owned property on the outskirts of the Talladega National Forest.

Table 3.1: Details of the reference stand maps used in this study. Stands can be highly variable in their area, as highlighted in the high standard deviation across all stand maps

| Study Area | No. of Stands | Total Area (ha) | Mean | Stdev |
|---------------------------|---------------|-----------------|------|-------|
| Talladega National Forest | 6310 | 62087 | 9.7 | 12.1 |
| Talladega Outskirts | 41 | 566 | 13.3 | 27.5 |
| Whitehall Forest | 128 | 330 | 4.8 | 7.6 |

real stands (e.g., stands on the opposite sides of the roads are distinct, by species or age or just based on the fact that they are split by the road). This further informs the idea that management units and practices can be based on many different considerations, not necessarily observed through CHM or species statistics.

The mean stand size is around 4.8 ha with a standard deviation of 7.6 ha.



Figure 3.3: Reference stand map for the Whitehall Forest.

CHAPTER 4

AUTOMATED STAND DELINEATION – HOMOGENEITY-BASED APPROACH

This chapter presents a strategy of automatically generating and evaluating stand maps. For any automated method of performing a task, there must be a method of evaluating the quality of its results. Section 4.1 is dedicated to discussing some ways in which stand maps have been quantitatively judged. We carefully examine the effectiveness of these metrics and discuss some of the results obtained using the reference maps and the study areas described in the previous chapter. Section 4.2 then provides a workflow within ArcGIS Pro that can be used to maximize the homogeneity of a chosen property of stands. We also present a method of masking riparian zones. Such zones are highly prevalent and problematic when delineating a landscape such as the Talladega National Forest.

4.1 Evaluation Metrics

Evaluation strategies can be categorized into two types: supervised and unsupervised. A supervised method is one that relies on reference or ‘ground-truth’ data. The output of the algorithm is directly compared to the reference. In the case of stand delineation, these metrics typically consider the overlaps between stand polygons generated by the algorithm and the corresponding stands in the reference stand maps (i.e., those drawn by human experts). On the other hand, unsupervised methods of evaluation are typically used to judge the clustering quality of the data. In our use case, unsupervised metrics evaluate the intrastand homogeneity and the interstand heterogeneity of the generated stand maps with respect to characteristics such as tree volume and basal area.

4.1.1 Supervised Methods

Several metrics have been proposed for the evaluation of segmentation results with respect to a given ‘ground truth’ delineation. A pair of reasonable metrics comparing the overlaps between generated and reference stands were proposed by Ke et. al [12]. These are: (1) the relative area of an overlapped region to a reference object ($RA_{or}\%$); and (2) the relative area of an overlapped region to a segmented object ($RA_{os}\%$). Equations for both are shown below.

$$RA_{or}\% = \frac{1}{n} \sum_{i=1}^n \frac{A_o(i)}{A_r} \times 100 \quad (4.1)$$

$$RA_{os}\% = \frac{1}{n} \sum_{i=1}^n \frac{A_o(i)}{A_s(i)} \times 100 \quad (4.2)$$

Here, n is the number of objects of interest, where an object of interest is an overlapping region that covers at least 10% of a reference polygon, $A_o(i)$ is the area of the i^{th} overlapped region associated with a reference polygon, A_r is the area of the reference polygon, $A_s(i)$ is the area of the i^{th} object of interest.

An oversegmented image will result in a low $RA_{or}\%$ value and a high $RA_{os}\%$ value. An undersegmented image will exhibit a high $RA_{or}\%$ value and a low $RA_{os}\%$ value. Ideally, both metric values should be equal and high (Figure 4.1).

The second metric that we employ is the *intersection over union* (IoU). The IoU is a commonly implemented metric across all types of segmentation/object-based image analysis tasks. In the context of forest management, Xiong et. al. [8] employed the IoU to evaluate the quality of their stands, and they claim that for an individual stand, an $\text{IoU} > 0.5$ showcases good agreement and an $\text{IoU} > 0.7$ implies very good agreement with the reference stand. The IoU between two polygons X and Y, is defined as follows:

$$\text{IoU} = \frac{A(X) \cap A(Y)}{A(X) \cup A(Y)} \quad (4.3)$$

The IoU metric is generally used to compare a single pair of objects. Due to the ‘mosaic-like’ nature of stand maps, it may be difficult to establish a strong one-to-one paring between a reference stand and a generated stand, as a reference stand may overlap with multiple generated stands. To address this issue, our implementation in this study centers the metric around the reference map. Therefore, for each reference

stand, only the generated stand that has the highest IoU is considered to be its pairing. The average IoU for a generated stand map is thus the average of the highest IoUs obtained for each reference stand.

Unsupervised Methods

Unsupervised methods of evaluation are based on the output exhibiting useful patterns and information without reference to any external ground-truth. As management policies and planned activities are assigned to entire stands, it is necessary that the stand must be as homogeneous as possible. To avoid redundancies with having to manage an excess of small stands, it is also important that neighboring stands be sufficiently different in characteristics. Unsupervised methods of evaluation help us analyze the effectiveness of a generated stand map on these two aspects with respect to the required characteristics.

One popular approach of measuring the goodness of a delineation is by evaluating the degree of variance in a metric which was explained by the delineation (R^2) [18][17]. The R^2 statistic is calculated as follows:

$$R^2 = 1 - \frac{SSE}{SST} \quad (4.4)$$

$$SST = \sum_{j=1}^N \sum_{i=1}^{n_j} (z_{ij} - \bar{z})^2 \quad (4.5)$$

$$SSE = \sum_{j=1}^N \sum_{i=1}^{n_j} (z_{ij} - \bar{z}_j)^2 \quad (4.6)$$

where N is the number of polygons/stands in the delineation, SSE stands for the sum of squares error, SST stands for the total sum of squares, n_j is the number pixels in polygon j , z_{ij} is the value of the pixel

i lying in polygon j , \bar{z} is the mean pixel value of the raster over the entire area, and \bar{z}_j is the mean value of all the pixels that lie in polygon j .

R^2 has been used frequently across studies to assess the explainability of tree height, DBH and other characteristics by a generated segmentation. We perform our experiments around R^2 with respect to tree volume, basal area and CHM. An ideal R^2 value is close to 1, indicating consistency within the stand and variance among neighboring stands. However, R^2 does tend to favor smaller, trivial stands as will be discussed later.

Another metric used to maximize intersegment heterogeneity and intrasegment heterogeneity is the *Global Score*, introduced by Johnson and Xie [11]. The Global Score serves as measure of detectability of separation of regions and of homogeneity within regions. To fix some of the inconsistencies that may occur, normalized versions of the weighted variance and Moran's Index were introduced by Bock et. al [22] and used in the experiments performed by Sanchez-Lopez et al. [21]

The inter-segment heterogeneity is measured by Moran's Index:

$$MI = \frac{\sum_{i=1}^n \sum_{j=1}^n w_{ij} (y_i - \bar{y})(y_j - \bar{y})}{(\sum_{i=1}^n (y_i - \bar{y})^2) (\sum_{i \neq j} w_{ij})} \quad (4.7)$$

where y_i and y_j are the mean values of the metric in polygons i and j respectively, \bar{y} is the mean value of the metric/raster, and w_{ij} is a matrix that defines $w_{ij} = 1$ if polygons i and j are adjacent and $w_{ij} = 0$ if not. MI values close to 1 reflect high spatial autocorrelation, values close to 0 represent random patterns and values close to -1 represent low spatial correlation.

The intra-segment homogeneity is measured by the weighted variance (Wvar)

$$WVar = \frac{\sum_{i=1}^n a_i v_i}{\sum_{i=1}^n a_i} \quad (4.8)$$

v_i is the variance of polygon i , a_i is the area of polygon i and n is the total number of polygons.

The normalized versions of the metrics are presented as follows :

$$WVar_{norm} = \frac{Wvar}{y'} \quad (4.9)$$

$$MI_{norm} = \frac{MI + 1}{2} \quad (4.10)$$

As for the Global Score itself, it is defined using both inter-segment heterogeneity and intra-segment homogeneity.

$$GS_{mod} = \sqrt{\frac{(WVar_{norm}^2 + MI_{norm}^2)}{2}} \quad (4.11)$$

where $WVar_{norm}$ is the normalized weighted variance of the raster band values in the segments (y' is the overall variance of the image/raster), MI_{norm} is the normalized Moran's index that measures inter-segment heterogeneity. GS_{mod} thus ranges from 0 to 1, with values closer to 0 representing the ideal case, with high intrasegment homogeneity as well as high intersegment heterogeneity.

We present our study with the use of the R^2 , GS ($WVar$ & MI) as our unsupervised metrics and IoU, $RA_{or\%}$, $RA_{os\%}$ as our supervised metrics. Both R^2 and GS serve a similar purpose in helping us directly understand the quality of a segmentation. The traditionally employed R^2 metric does, however, tend to

favor much smaller, trivial polygons and thus must be coupled with the area/number of desired polygons constraint. As GS is a combination of W_{Var} and MI, it is more robust and does not favor such trivial solutions (Fig 4.6).

On the other end, an overlap-based supervised metric like IoU is very commonly used in object-based image analysis tasks across various domains. While the overall effectiveness of comparing generated delineations to ‘ground-truths’ is questioned in the further sections, Xiong et. al. [8] suggested an effective way of using this metric for a task such as stand delineation, where the proportion of well-delineated polygons is presented. The combination $RA_{or\%}$ and $RA_{os\%}$ also ensures that there is a healthy balance between oversegmented and undersegmented stands 4.5.

4.2 Methodology

We now present a strategy for efficient creation and evaluation of stand maps. The main idea behind this methodology is to provide a quick and effective way of generating stand maps, one that gives the user the ability to prioritize the homogeneity of their chosen stand characteristics. The user can then find a balance between the strictness with which homogeneity must be preserved and how much freedom is allowed in an effort to achieve feasible, large stands.

Before we move on to the primary methodology, we present a pre-processing step for identifying streams and masking riparian zones. This step is especially useful for a region such as the Talladega National Forest, where riparian zones make up much of the area and play a significant role in separating stands. Delineating riparian zones in particular can be challenging for stand delineation algorithms. Thus, we

mask away these zones first. This step may or may not be necessary, depending upon the area to be delineated.

First, we get rid of the minor sinks and imperfections in the DEM using the Fill tool from the hydrology tools in ArcGIS Pro. A sink is a tiny depression in the topography, where water flowing into it would accumulate over time. The 'fixed' DEM is then treated to the Flow Direction tool with the D8 algorithm. The D8 algorithm assigns the flow direction of a pixel to its steepest downslope neighbor.

With this flow direction raster, we calculate the accumulated flow using the flow accumulation hydrology tool. With this, we obtain a raster with very high values along the pixels where the maximum flow accumulates. These pixels presumably represent the streams in the area. Then, by creating a 50 meter buffer along the pixels that have a flow accumulation > 1000 (representing streams), we can get a good estimate of the riparian zones, as presented in Figure 4.7 .

The Mean Shift Segmentation Tool in ArcGIS Pro is primarily used to create an initial delineation. The tool requires a single-band or a 3-band raster as its input. The parameters for the segmentation are the (1) spectral detail (pixel value importance) value ranging from 1 to 20, (2) spatial detail (proximity importance) value ranging from 1 to 20, and (3) minimum segment size (this parameter does not seem to enforce a strict lower bound; it can be considered as a 'scale' parameter instead). We performed our experiments with the spatial and spectral details set to 20, the highest possible value. We do this to ensure that the segments/clusters generated are highly specific. At this stage, we prioritize the homogeneity of the microstands. Similar enough clusters will eventually be merged in the subsequent steps.

One of the primary advantages of this tool is that it is computationally efficient and can generate an initial delineation for very large rasters quickly. A downside of using just this method is that there is a larger

variance in the sizes of the polygons generated when we wish to ensure a large minimum size for our stands. Another downside is the limit on the number of bands which can be used to segment the rasters, along with the inability to assign weights/importance to some bands over others.

Therefore, we only use this tool as an initial step to generate small polygons which can be treated as ‘super pixels’. We then iteratively merge these polygons based on the similarity in the zonal statistics with respect to the chosen criteria. As the initial polygons are very small, we allow greater freedom for merging by having a large merge threshold. The threshold becomes tighter with each iteration, ensuring that large polygons may only merge if they are very similar. The initial threshold and the rate at which the threshold lowers can be set by the user. The user can iteratively merge the nearest neighbors with the similarity function using the mean CHM value until all stands surpass the minimum area constraint. The user can then experiment with different kinds of similarity functions and initial parameters.

It is also possible to create a single composite band using a weighted sum of multiple raster layers. The weights can be considered as another set of parameters to be adjusted for optimal results. We did experiment with doing this, but we did not achieve any better results using these composite layers. Our best results were obtained using just a single band, CHM [12][16].

Algorithm 1 ArcGIS-Based Segmentation and Polygon Processing

- *spec*: Spectral detail parameter
- *spatial*: Spatial detail parameter
- *min_size*: Minimum segment size
- *initial_layer*: Input raster layer (1 or 3 bands)
- *dissolve_itr*: Iterations of Similarity based merges
- *elim_size* = 5000: Elimination area threshold for small polygons (m²)
- *merge_threshold*: %Similarity threshold to merge neighboring polygons
- *diss_layer*: Raster Band for Similarity Evaluation for merging

begin

Initial Segmentation

1. (Optional) Mask riparian areas: $\text{initial_layer} \leftarrow \text{Con}(\text{rip_mask} = 1, 0, \text{initial_layer})$
2. Mean Shift segmentation: $\text{seg_raster} \leftarrow \text{MSS}(\text{initial_layer}, \text{spec}, \text{spatial}, \text{min_size}, \text{bands})$

Vector Conversion

1. Convert raster to polygons: $\text{RasterToPolygon}(\text{seg_raster}, \text{"results.shp"})$
2. Calculate polygon areas: $\text{CalculateGeometryAttributes}(\text{"Shape_A"}, \text{"AREA"})$

Small Polygon Elimination for 3 iterations do

1. Select small polygons: $\text{SelectLayerByAttribute}(\text{"Shape_A"} < \text{elim_size})$
2. Eliminate by length: $\text{Eliminate}(\text{selected}, \text{"results.shp"})$

Dissolve Iterations for each $\text{itr} \in 1$ to dissolve_itr do

1. Calc zonal stats: $\text{zone_stats} \leftarrow \text{ZonalStatisticsAsTable}(\text{diss_layer}, \text{"MEAN/MEDIAN/STD"})$
2. Join statistics to polygons: $\text{Join}(\text{"FID"}, \text{zone_stats}, \text{results.shp})$
3. Find polygon neighbors: $\text{PolygonNeighbors} \rightarrow \text{neighbors.dbf}$
4. **Merge Criteria: for each neighbor pair do**
 - if** $\frac{|\text{src_MEAN} - \text{nbr_MEAN}|}{\text{src_MEAN}} \leq \text{merge_threshold}$ **then**
 - Mark to merge
5. **Merge marked polygons**

Return Final polygon layer (results.shp)

Table 4.1: Relative Overlaps of reference stand maps created by experts at the Warnell School of Forestry and Natural Resources and the USDA forest service. This highlights the subjectivity in delineation of stand maps. Although, there are stands where there is good alignment, minor changes can cause a ripple effect in the overall stand maps, which is reflected in the highly sensitive nature of the supervised metrics.

| IoU | $RA_{or}\%$ | $RA_{os}\%$ |
|------|-------------|-------------|
| 0.37 | 38.8 | 44.46 |

4.3 Results and Discussion

We first examined the reference stand maps over different regions by evaluating R^2 and GS_{mod} values with respect to variables such as the CHM, tree volume, etc. (Figure 4.9). The reference maps for each study area were created independently by different experts. Maps were created using optical imagery. Other constraints which the experts might have considered were not specified.

We also analyzed two independently-created stand maps, both created by experts. These were evaluated by treating one of the maps as the reference or ‘ground-truth’. The results, seen Table 4.1, were relatively poor, highlighting the subjectivity in the creation of stand maps for a difficult landscape. This subjectivity likely arises due to management constraints that are not explicitly specified or due to other implicit factors that are not decipherable through imagery.

The differences in the values Figure 4.9 and Table 4.2 highlight the difficulty in creating homogeneous stands in relationship to the complexity of the landscape. The topography, as seen with the DEM, plays a much bigger role in the interiors of the Talladega National Forest. This is most likely due to the fact that Talladega is a natural forest, unlike the plantation/managed forests typically used in research.

The Talladega National Forest is a natural, unmanaged forest with a complex landscape. We have two reference stand maps, created independently by experts, covering large forest areas. A preliminary visual

Table 4.2: Values of unsupervised metrics of stand maps created by experts. GS_{mod} is a combination of W_{var} and MI_{norm} , ideally having low values. R^2 values should be higher ideally.

| Study Area | Layer | W_{var} | MI_{norm} | GS_{mod} | R^2 |
|---------------------|--------|-----------|-------------|------------|-------|
| Talladega Interior | CHM | 0.82 | 0.42 | 0.65 | 0.17 |
| | Volume | 0.66 | 0.43 | 0.55 | 0.31 |
| | DEM | 0.42 | 0.59 | 0.51 | 0.57 |
| Talladega Outskirts | CHM | 0.66 | 0.42 | 0.55 | 0.33 |
| | Volume | 0.56 | 0.44 | 0.50 | 0.43 |
| | DEM | 0.51 | 0.74 | 0.63 | 0.48 |
| Whitehall | CHM | 0.46 | 0.49 | 0.48 | 0.53 |
| | Volume | - | - | - | - |
| | DEM | 0.20 | 0.72 | 0.53 | 0.79 |

inspection of the reference stands indicates issues that make the area especially challenging for human experts and more so for algorithms with lesser semantic information. The presence of a large proportion of multi-species stands decreases the homogeneity within and makes it harder to enforce strict boundaries between neighboring stands. There also exist very large polygons representing riparian zones extending across the forest. These large, long polygons are significant outliers in terms of the typical shape and size of a stand. An algorithm is thus prone to over-segmenting these stands, and this effect is amplified in our IoU-like metrics which are weighted by the relative areas of the polygons.

The R^2 scores of expert delineations in Talladega National Forest are fairly low. This is likely due to 1) the highly heterogeneous landscape 2) management constraints not readily apparent through LiDAR data or optical imagery and 3) the stock variable maps being themselves imputed. Under such circumstances, it may be inappropriate to use IoU-like metrics to judge the quality of a delineation, where the ‘ground-truth’ reference map itself is subjective.

CHM-based results proved to be the most visually appealing as well as being consistent with the reference maps and the overall explainability of tree volume, an essential stock variable in gauging stand

Table 4.3: Obtained results over Whitehall with respect to the reference map. Note that GS and R^2 values are reported with respect to the CHM. Outputs visualized in Figure 4.12.

| Map | IoU | $RA_{or}\%$ | $RA_{os}\%$ | GS | R^2 |
|--------------------|------|-------------|-------------|------|-------|
| Reference | - | - | - | 0.48 | 0.53 |
| Generated Map | 0.24 | 0.29 | 0.45 | 0.39 | 0.74 |
| Reference (masked) | - | - | - | 0.57 | 0.74 |
| Generated (masked) | 0.39 | 58.1 | 55.2 | 0.55 | 0.82 |

revenue. These results are highlighted in Figures 4.10 and 4.11. The results were categorized into ‘small’ and ‘large’ stands in reference to the work by Pukkala et. al.[26]. ‘Small’ stand maps contain stands which are not yet acceptable as a current stand size standard, yet ones that maximize explainability of volume and could be used as a form of management units in the future. ‘Large’ stands are those that are close to the stands that we see in the reference maps in terms of acreage. Our results show better explainability of variance in volume over both areas with respect to the reference maps, while still being practical. Note that this experiment is done over a smaller 500 hectare area in Talladega. Other overlap based concerns were disregarded, only the relative sizes were of concern. We also note that due to the ‘easier’ landscape in the outskirts of Talladega, all metrics reflected better values.

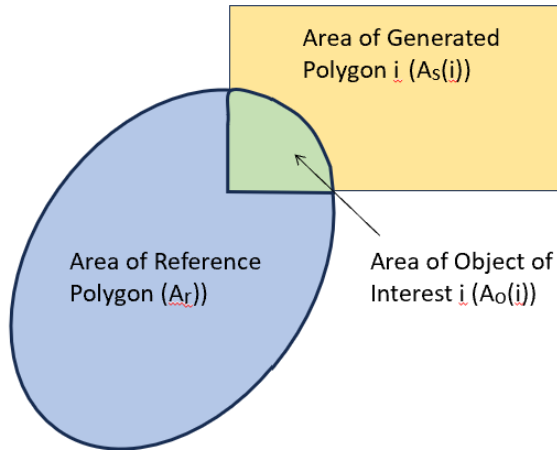
The decision-making process behind the Whitehall stand map involved considering electrical power lines and interior roads as separate polygons. These are known by experts but not clearly visible on lower resolution aerial images and LiDAR. We present our results in Table 4.3 and Figure 4.12, where our algorithm could not detect some of the roads that were obscured by the canopy, leading to lower values in the intersection-based metrics. Most of the other stands however, seem to be visually well aligned with the reference. We observe much better homogeneity scores with respect to the CHM in the generated map.

Table 4.4: Obtained results after masking riparian zones. Outputs visualized in Figure 4.13

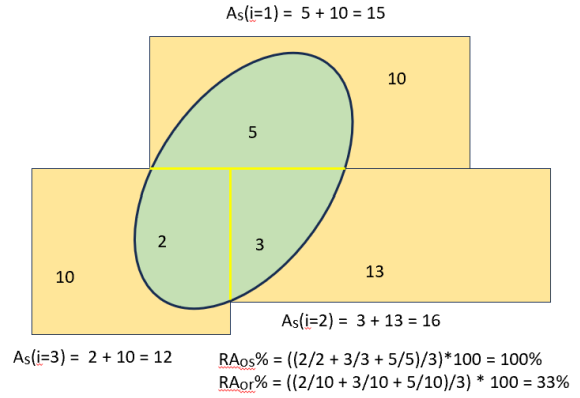
| Map | IoU | $RA_{or}\%$ | $RA_{os}\%$ | GS | R^2 |
|--------------------|------|-------------|-------------|------|-------|
| Reference | - | - | - | 0.56 | 0.32 |
| Generated Map | 0.27 | 31.2 | 36.5 | 0.55 | 0.35 |
| Generated (masked) | 0.25 | 35.1 | 40.2 | 0.60 | 0.30 |

To address the issues of riparian zones interfering with the workings of our algorithm, we present some of the results using our masking process as shown in Figure 4.13 and Table 4.4. Note that the scale parameters for the delineation change significantly as a big portion of the raster is masked out. We observe slightly worse homogeneity results with respect to the tree volume. However, the final stand map is much more visually aligned with the reference map as compared to the previous ‘Large’ stand map.

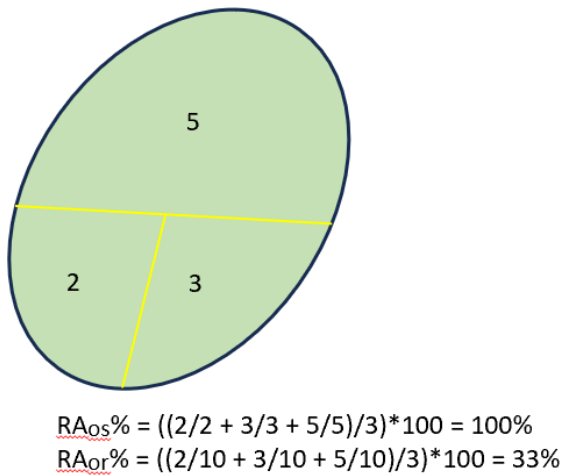
It is clear that stand maps can be very subjective and the decision to delineate certain polygons are not always clearly represented in the imagery. The decision to split roads or forest management regulations such as having a buffer zone near water bodies (riparian zones) are some examples where a rigid, objective approach to stand delineation does not apply. The ripple effect of delineating a single stand incorrectly can affect the entire stand map, and thus the intersection-metrics. In the next chapter, we present a more hands-on, semi-automated approach to stand delineation, one which better takes these realities into consideration.



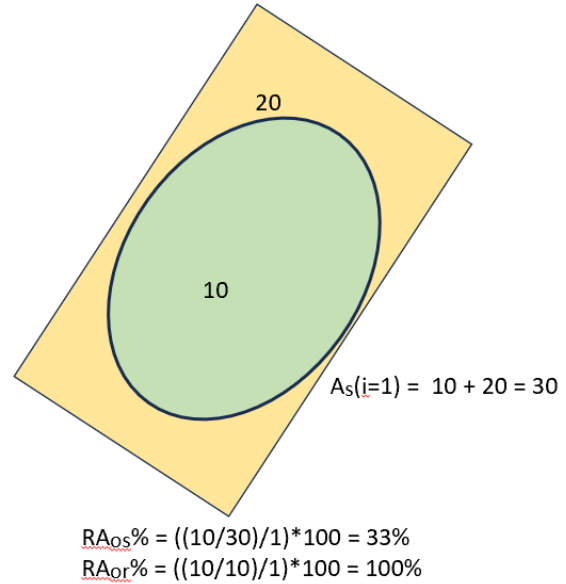
(a) Legend. Object of interests are overlapping segments covering at least 10% of the reference polygon area.



(b) Typical, non-ideal case. Three overlapping regions, resulting in low $RA_{or}\%$ and $RA_{os}\%$ values.



(c) Oversegmented Polygon. High $RA_{os}\%$, low $RA_{or}\%$.



(d) Undersegmented polygon. Low $RA_{os}\%$, high $RA_{or}\%$.

Figure 4.1: Cases of overlaps and reflected $RA_{or}\%$ and $RA_{os}\%$ values. A better segmentation would yield higher and more equal $RA_{or}\%$ and $RA_{os}\%$ values. Numbers in colored regions indicate area (units unspecified).

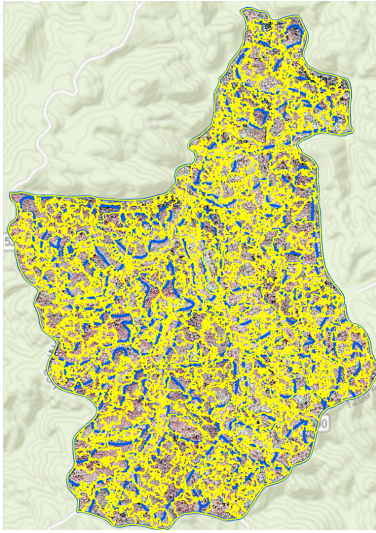


Figure 4.2: Oversegmentation
(IoU = 0.09, $RA_{or}\%$ = 21.8,
 $RA_{os}\%$ = 52.9)

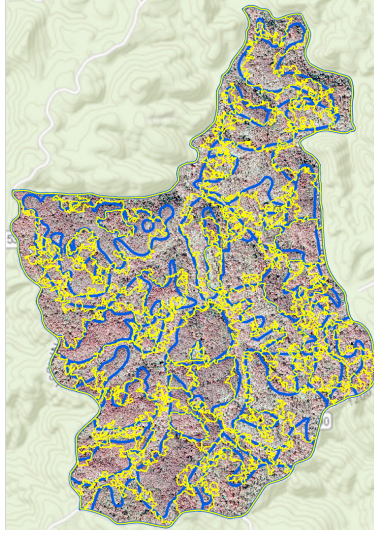


Figure 4.3: Good Segmentation
(IoU = 0.39, $RA_{or}\%$ = 42.4,
 $RA_{os}\%$ = 43.1)

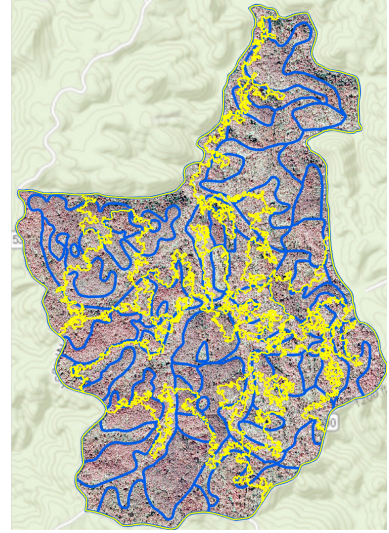
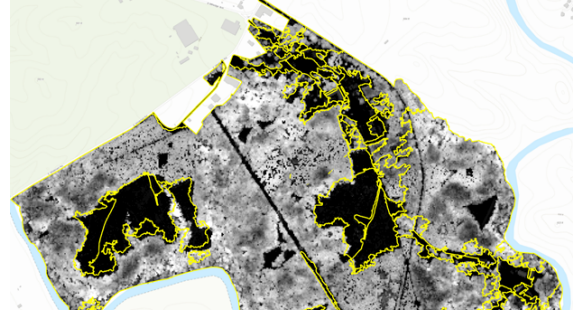


Figure 4.4: Undersegmentation
(IoU = 0.22, $RA_{or}\%$ = 58.3,
 $RA_{os}\%$ = 24.8)

Figure 4.5: Visualizing the effects of supervised metrics (Generated polygons in yellow, reference polygons in blue). $RA_{or}\%$ favors larger polygons, $RA_{os}\%$ favors smaller polygons. An ideal segmentation achieves a good balance.



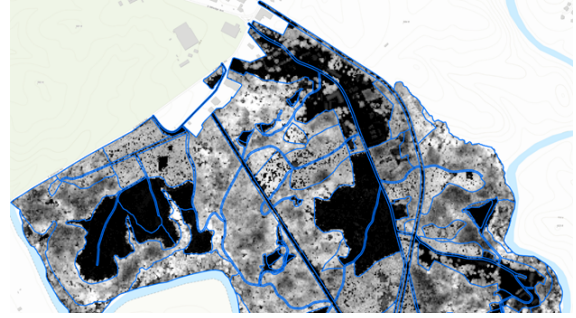
(a) $wVar_{norm} = 0.37$; $MI_{norm} = 0.85$; $GS_{mod} = 0.65$; $R^2 = 0.62$



(b) $wVar_{norm} = 0.63$, $MI_{norm} = 0.63$, $GS_{mod} = 0.63$, $R^2 = 0.36$



(c) $wVar_{norm} = 0.30$, $MI_{norm} = 0.53$, $GS_{mod} = 0.43$, $R^2 = 0.69$



(d) $wVar_{norm} = 0.46$, $MI_{norm} = 0.49$, $GS_{mod} = 0.48$, $R^2 = 0.52$

Figure 4.6: Segmentations overlayed and evaluated on CHM. Values range from 0-1. Ideally, $wVAR_{norm}$, MI_{norm} , GS_{mod} values should be close to 0. R^2 values should be closer to 1. Figure 4.6(a) is an example of highly homogeneous segments (low $wVAR_{norm}$) but low heterogeneity between neighboring segments (high MI_{norm}). 4.6(b) shows low intra-segment homogeneity (high $wVAR_{norm}$). Figure 4.6 (c) is a relatively good segmentation with high intra-segment homogeneity (low $wVAR_{norm}$) and high inter-segment heterogeneity (low MI_{norm}). Figure 4.6 (d) highlights the metric values of the reference delineations. Although the reference map might not necessarily reflect the best values, it is important to note that the metrics are only based on the CHM here.

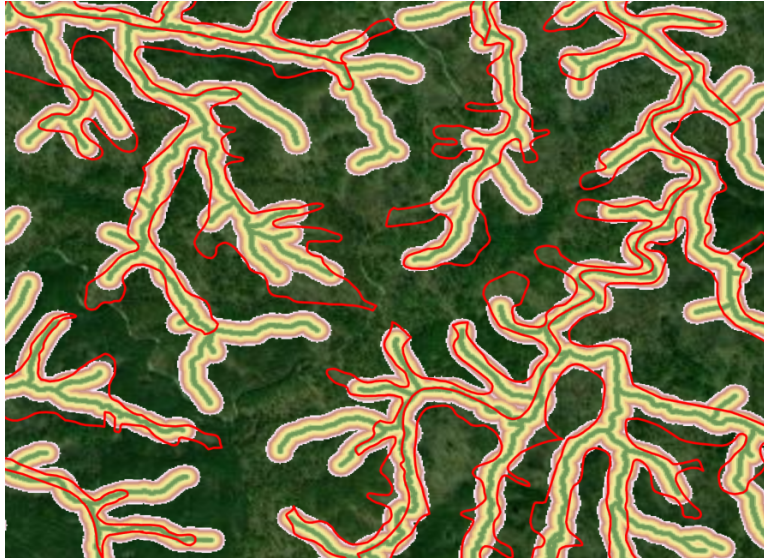


Figure 4.7: Derived riparian zones using Hydrology tools within ArcGIS Pro. Polygons with red borders describe the riparian zones delineated by experts.

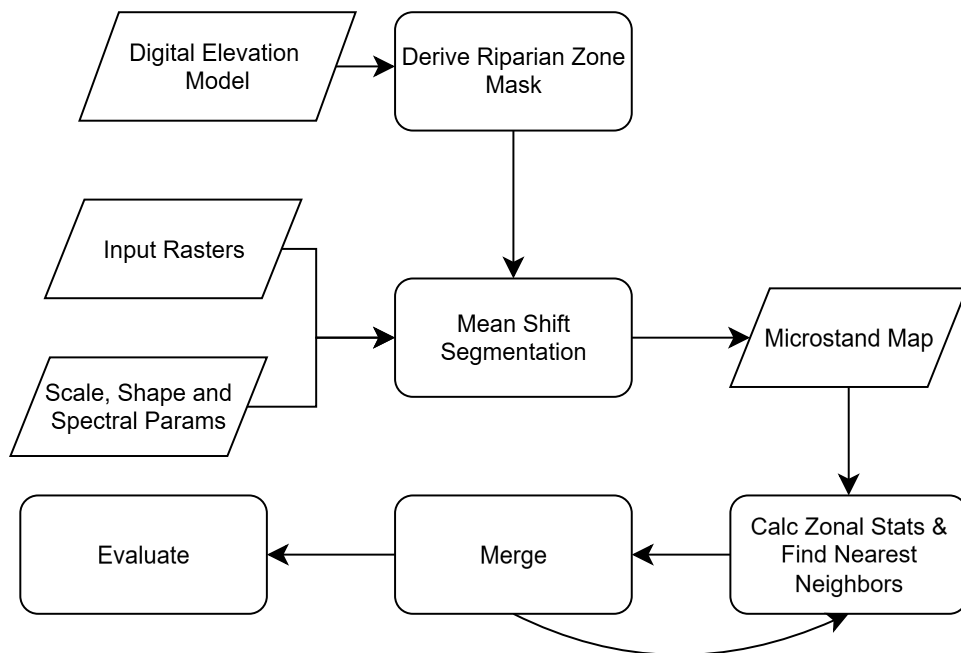


Figure 4.8: Overview of delineation methodology using ArcGIS Pro

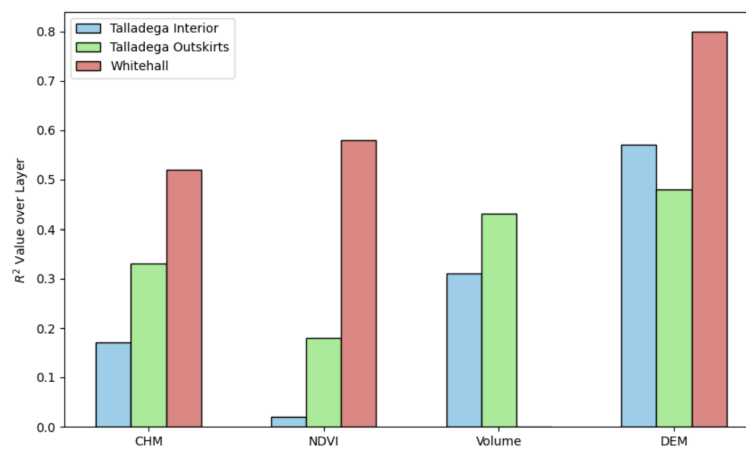
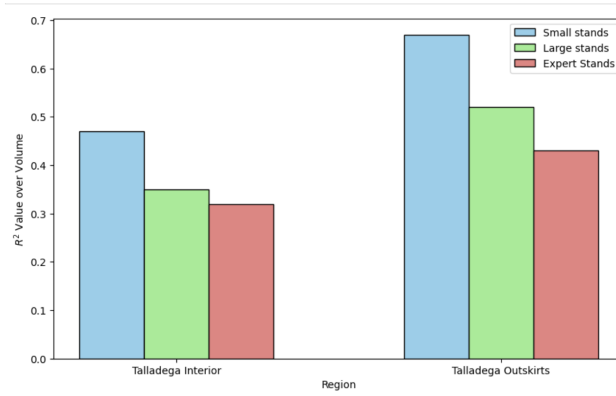
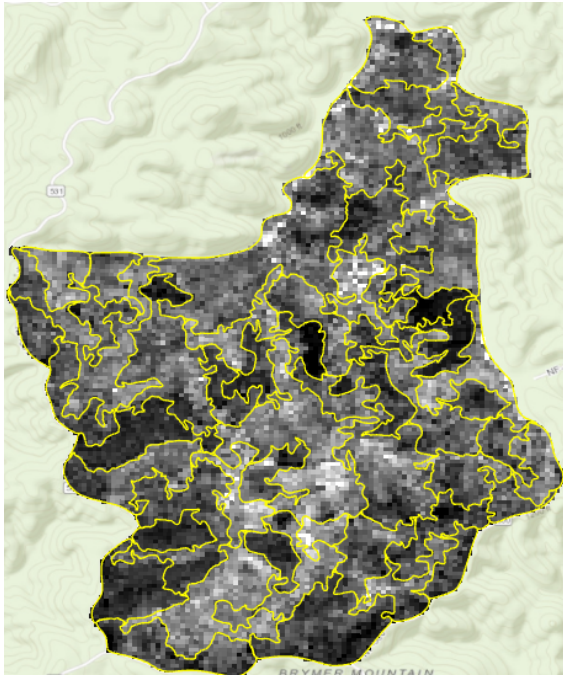


Figure 4.9: Segmentations created by independent experts in three different regions. The figure highlights the difficulty of creating stand maps based on the landscape. The CHM provides direct information about tree height and is useful for experts to create stand maps. Tree volume is an important stock variable that must be explained well by good delineations. NDVI is useful for differentiating vegetation cover types. Whitehall (a well-managed research forest) seems to be the delineated well across all metrics. This is followed by the Outskirts of Talladega (private land), followed by the Interiors of the Talladega National Forest.

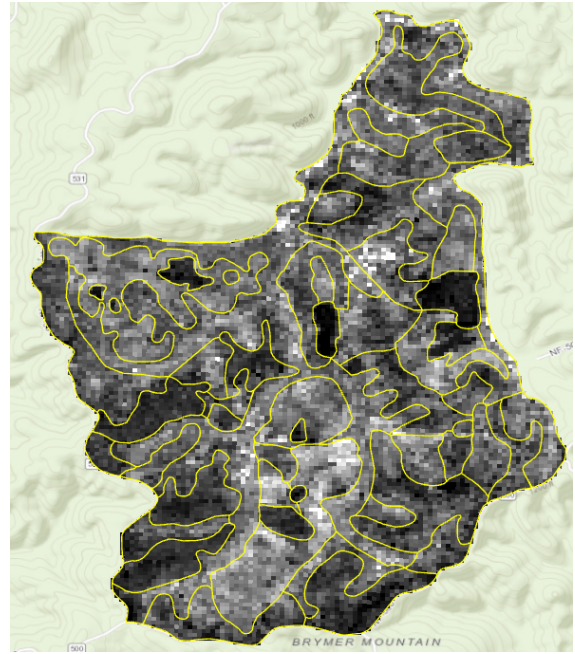


| Region | Delineation Type | # Stands | Avg Stand Size (ha) | R^2 |
|---------------------|------------------|----------|---------------------|-------|
| Talladega Interior | Small Stands | 227 | 1.9 | 0.47 |
| | Large Stands | 51 | 8.6 | 0.35 |
| | Reference | 53 | 8.3 | 0.32 |
| Talladega Outskirts | Small Stands | 238 | 2.3 | 0.67 |
| | Large Stands | 43 | 12.8 | 0.51 |
| | Reference Stands | 41 | 13.6 | 0.43 |

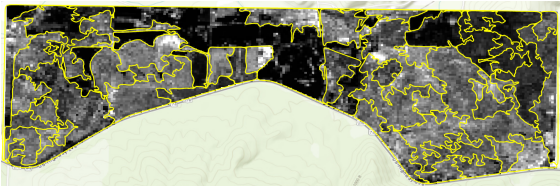
Figure 4.10: Two scales were chosen for delineation. Small stands are representative of highly homogeneous areas that are reasonably sized based on the work of Pukkala et. al. [26]. The scale for large stand delineations was selected to closely match the number of reference polygons. For both scales and regions, the algorithmic delineations show better explainability over tree volume.



(a) Talladega Interior: 'Large' Delineations



(b) Talladega Interior: Reference Map



(c) Talladega Outskirts: 'Large' Delineations



(d) Talladega Outskirts: Reference Map

Figure 4.11: CHM based delineations, overlaid on volume maps as discussed in 4.10.

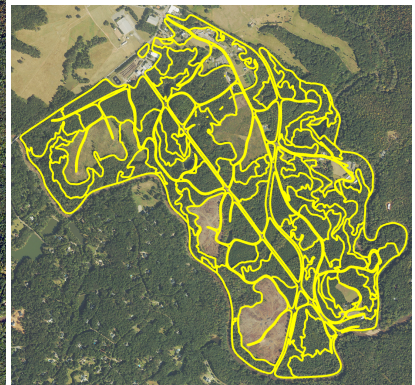
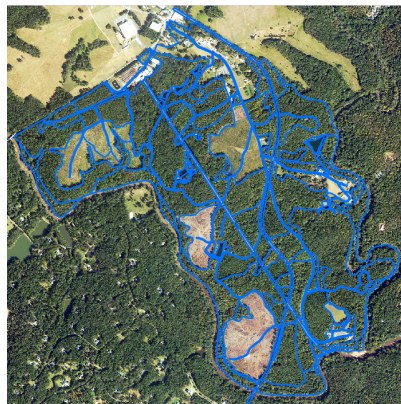
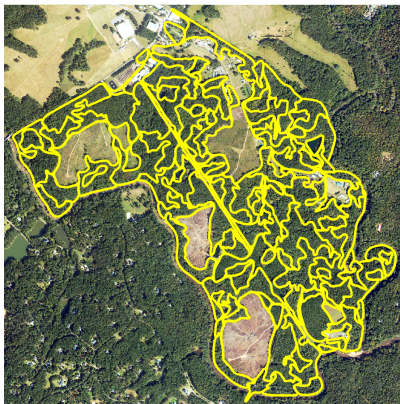


Figure 4.12: Whitehall map derived from our methodology (left) and derived map after masking roads (right), compared to reference map (center), as presented in Table 4.3.

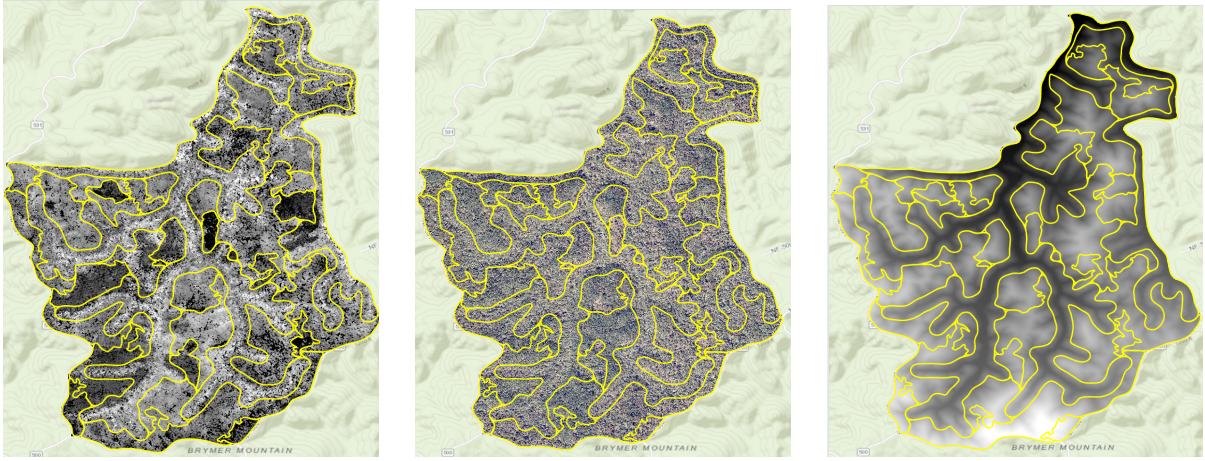


Figure 4.13: Segmentation created by initially masking derived riparian zones. Overlayed on CHM (left), natural image (center) and DTM (right). Evaluation based on Volume: $W_{var} = 0.68$; $MI_{norm} = 0.5$; $GS_{mod} = 0.6$; $R^2 = 0.3$; $RA_{or\%} = 35.1$; $RA_{os\%} = 40.2$; $IoU = 0.25$.

CHAPTER 5

HUMAN-INVOLVED APPROACH

We discussed the limitations of fully automated approaches to stand delineation in the previous chapter. A fully automated method requires a well-defined objective function to optimize. A stand map requires homogeneous units in terms of tree species, mean DBH and age, while also taking the topography and forest management regulations into account. There does not seem to be a one-size-fits-all model to delineate stands due to the varying characteristics and complexities of forest landscapes. There also exists subjectivity in delineations among experts.

Because of this, in this chapter we present a method attempting to capture user preferences and implicit considerations. The method requires the expert to provide some sample stands to learn from, while also providing an easier way of creating said sample stands.

5.1 Methodology

The process for generating a delineation is broken into three distinct steps. The first step consists of automatically generating a microstand map, which creates highly homogeneous yet impractically small stands. Under the hood, there is another microstand map with larger stands that is generated simultaneously; it provides additional context for the final model. This leads into the second step, where the user would select the microstands that should be merged to create a stand. These would then form the sample, user-created stands that the algorithm would learn from. The third step requires users to provide rasters such as the CHM and DEM. These rasters, along with the created sample stands, inform the underlying random forest algorithms about the thresholds relating to the microstand statistics that were implicitly considered by the user when they decided to select or ignore a microstand to be merged with its neighbor. Using these learned thresholds, the random forest algorithm looks at every pair of microstands and decides if they must be merged together. The final stand map is thus generated.

The following subsections describe the inner workings of this process and the custom-made tools implementing them in ArcGIS Pro. The overall objective is to simplify the stand-delineation process for end users.

5.1.1 Generating Microstands

The first step in this method is similar to the one discussed in the previous chapter. We first oversegment the area using the Mean Shift Segmentation Tool in ArcGIS Pro, with the input typically being a single band raster (e.g., CHM) or a three band raster (e.g., a natural color image). We can also use a custom composite 3 band raster consisting of CHM, DEM and NDVI bands. As we want our initial stands to



Figure 5.1: Human-involved delineation - Step 1: Generate microstands

be small, we select a very low scale for the segmentation, around 5000. Another segmentation is created with the same inputs and parameters with the exception of scale, which is set to a higher value (approx. 10x) to create context stands (this is explained in the next subsections). It is also important to note that the segmentation tool outputs a raster, which we then convert to polygons using the raster to polygon tool. Unlike the previous methodology, no statistics or thresholds are calculated at this point.

5.1.2 Creating Sample Reference Stands

This step involves the user/expert. The user selects clusters of microstands they believe should be merged into proper stands. These stands then form the reference stands required for the algorithm to creating training datasets. This process should be done over multiple clusters. The number of reference stands that the user must provide versus the performance of the model is discussed in the next section. The user only

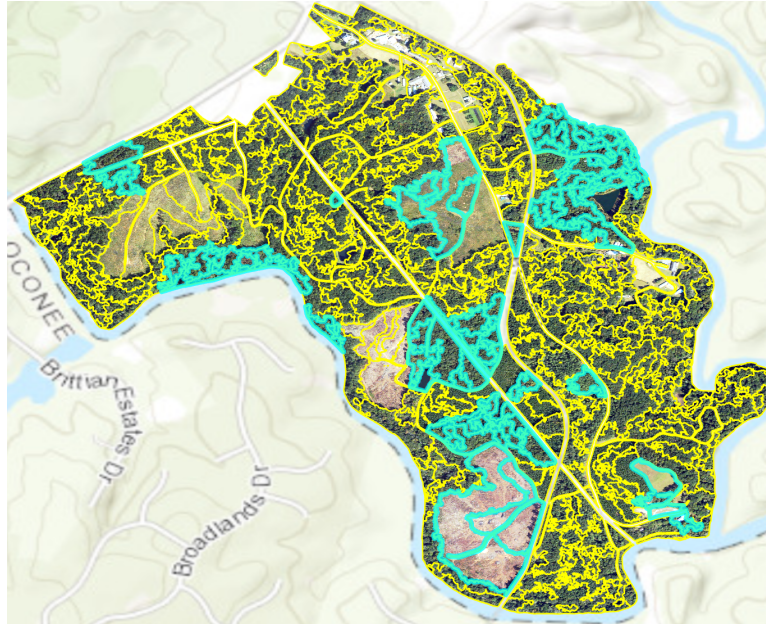


Figure 5.2: Human-involved delineation - Step 2: Create samples. Microstands highlighted in blue were chosen by the user to be merged

needs to perform a selection of the microstand polygons, instead of painstakingly drawing highly precise polygons in the ArcGIS Pro interface. Creating microstands over a raster like the CHM ensures that the non-redundant boundaries in the microstand map would be comparable to the ‘true’ stand boundaries. If the user already has an existing map consisting of some stands, they may be alternatively passed as an input to this tool. A spatial join would then be conducted, assigning microstands to the reference stands that they highly overlap with. With the same process, every microstand is also assigned a context ID, corresponding to the larger polygon in the context stand map that it belongs to. In either case, all the microstands that belong to or should belong to a single stand are assigned the same ‘expert IDs’.

5.1.3 Merging Microstands with Random Forest Classifier

The classifier looks at a pair of microstands, and predicts whether the pair should be merged or remain separate. First, we create our instances for the random forest. The user provides important rasters like the CHM, DEM, NDVI, green, red, blue, etc. bands. Zonal statistics like the mean, median, standard deviation, range, etc. are then calculated for each of the microstands for each available raster. The same statistics are also calculated for each of the context stands. The idea behind the context stands is to have a better understanding of the surrounding local region that a microstand lies in, under the same context in which the microstand was initially generated. The statistics of the context stands are attached to the microstands that they correspond to. Every pair of neighboring microstands thus becomes a training instance, with the features being the difference between the values for each of these statistics. The created sample stands help us create the training data labels for the Random Forest model. A pair of neighboring microstands that have the same expert ID form a positive instance (merge) whereas neighboring microstands that have different expert IDs (or one of them does not have an expert ID) form a negative instance (do not merge). The Random Forest classifier thus learns some of the characteristics and thresholds that determine whether a pair of microstands lie in the same ‘true’ stand. It then merges all the microstands that were predicted to belong to the same stand, creating the final output, tailored to the considerations of the user created sample stands.



Figure 5.3: Human-involved delineation - Step 3: Random Forest Merging + Smoothing

5.2 Results and Discussion

As one of the goals of this method is to save time and effort, we first examine our results over a large area in the Talladega National Forest, comprising approximately 2000 stands. We present our results with respect to the various strategies that an expert might go about sampling the ‘real’ stands.

Firstly, to maintain consistency among the experiments, we start with the same input parameters to generate identical microstand maps every time. As this approach is more holistic, the microstand map is not just created with a single band CHM raster. Instead, we create a composite 3-band raster, consisting of the CHM (structure), NDVI (species + density) and DEM (topography). The resulting microstand map thus consisted of 13,026 stands with an average area of approximately 1.6 ha and a standard deviation

Table 5.1: A comparison of the initial microstand map with the reference map for the larger Talladega area. The overlap metrics describe the oversegmented nature of the initial segmentation. The microstand map exhibits a significantly higher R^2 score with respect to the volume, likely due to the smaller average size of the polygons.

| Stand Map Type | IoU | $RA_{or}\%$ | $RA_{os}\%$ | No. of Stands | R^2_{vol} | GS_{vol} |
|----------------|------|-------------|-------------|---------------|-------------|------------|
| Reference | - | - | - | 2145 | 0.39 | 0.59 |
| Microstand | 0.10 | 23.37 | 54.92 | 13026 | 0.56 | 0.59 |

of nearly 1.4 ha. We present the microstand and reference map statistics in Table 5.1. The creation of this stand map took approximately 2 minutes.

The user must provide inputs such as the microstands with the polygons to be merged and the input rasters with which the zonal statistics will be calculated. Other hyperparameters that the end user would tune include the number of trees, the maximum tree depth, the minimum leaf size (or the cutoff number of samples at a node where it is considered a leaf node) and the probability threshold for predicted merges. In our experiments, the number of trees and the maximum tree depth have been set to 500 and 25, which are high but overall not as consequential with respect to time and performance based on our experiments. The hyperparameters that play a much bigger role are the minimum leaf size and the probability threshold. The minimum leaf size and the probability threshold determine the rigidity of the inference rules. For a very well trained model, the probability threshold will directly affect the degree of oversegmentation versus undersegmentation.

In the first user approach, we assume that the expert decided to create samples out of distributed compartments of stands around the forest. The way experts tackled the task of delineating Talladega was to first demarcate it into nearly 250 compartments. Each compartment contained approximately 40-50 stands. In the current scenario, 8 individual compartments were ‘delineated’ by the expert. The

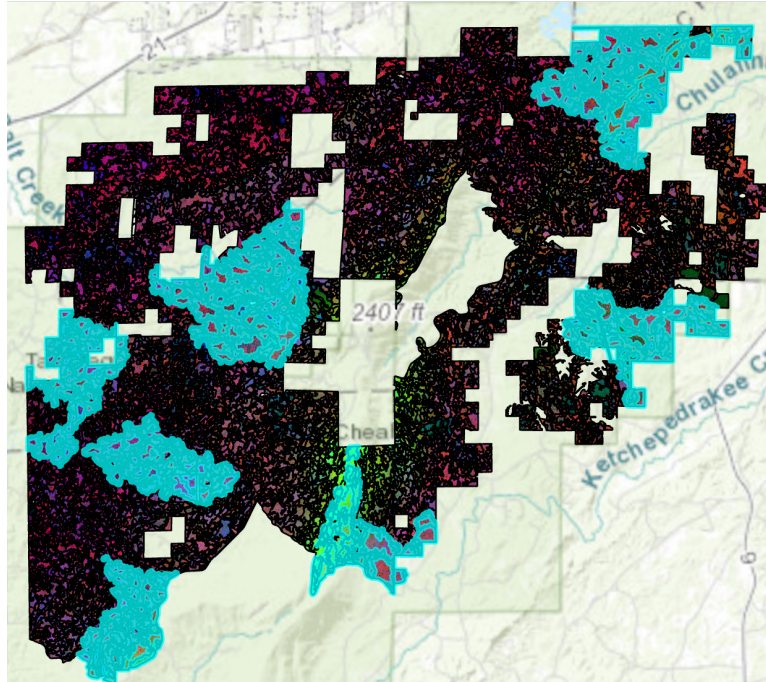


Figure 5.4: Nearly 450 stands created by the expert by merging microstands. Microstands merged over different ‘compartments’ within the study area.

delineation process was made easy, as the expert only needed to select the microstands needed to merge into proper stands. As such, nearly 450 ‘real’ stands were delineated by the expert as shown in Figure 5.4.

We present our results in Table 5.2. The average alignment of stands formed by merging microstands with those that were created on a blank canvas (i.e. the reference stands), was high, with an average IoU > 0.5 . At the highest probability threshold, the microstands that were merged by the random forest algorithm are highly reliable, although many of the microstands remained unmerged, resulting in a poor showing of the overall overlap metrics. At lower thresholds, microstands tend to overmerge, which can lead to large, unwanted stands that are difficult to process.

Before further discussion, we present our results with the second human strategy, where nearly 310 stands were delineated by the user, localized to a single area as shown in Figure 5.5, Table 5.3. The results

Table 5.2: Evaluation metrics for stands created by the human-involved approach, where 400 ‘real’ stands were formed across disjoint compartments in the larger Talladega region. As the leaf size is reduced and the probability threshold is increased, we observe a tighter enforcement of the inference rules established by the random forest model. This leads to poorer results on the overlap metrics, as the stands remain oversegmented. We see an improvement in the unsupervised metrics, as they tend to favor smaller segments. When we only consider the microstands that were merged to form stands by the user, we observe very good results in terms of overlaps. As the average IoU is > 0.5 , we can say that these user created stands are in good alignment with respect to stands that would have been drawn without the ease of just selecting microstands.

| Leaf Size | Probability Threshold | IoU | $RA_{or}\%$ | $RA_{os}\%$ | GS_{vol} | R^2_{vol} | No. of Stands |
|-----------|-----------------------|-------------|-------------|-------------|------------|-------------|---------------|
| 5 | 0.5 | 0.19 | 50.7 | 49.3 | 0.65 | 0.30 | 2442 |
| 5 | 0.6 | 0.17 | 35.4 | 49.6 | 0.59 | 0.46 | 5346 |
| 5 | 0.7 | 0.14 | 28.5 | 52.5 | 0.58 | 0.52 | 8904 |
| 5 | expert selected | 0.53 | 49.4 | 53.9 | - | - | 451 |
| 1 | 0.5 | 0.19 | 38.25 | 48.8 | 0.60 | 0.43 | 4400 |
| 1 | 0.6 | 0.15 | 30.7 | 51.2 | 0.58 | 0.50 | 7334 |
| 1 | 0.7 | 0.13 | 27.7 | 53.2 | 0.58 | 0.52 | 9692 |
| 1 | expert selected | 0.53 | 49.4 | 53.9 | - | - | 452 |

obtained were very similar to the ones obtained in the previous strategy. Possible explanations for this are that the overall complexity of the Talladega area makes it so that even localized compartments are just as heterogeneous as compared to two distant compartments. As the initial microstand map was the same in both cases, it may play a bigger role than anticipated. It is also likely that the random forest algorithm does not converge well enough to adapt to the study area. Regardless, the points made in the previous discussion, about the high quality of confidently merged microstands remain. Results with respect to the smaller sample area, used in the previous approach are also presented in Table 5.4. Here, the selected stands consisted of the bigger riparian zone polygon and five other disconnected stands.

For the Whitehall area, 18 out of the 134 ‘real’ stands were defined by the user. We observed significantly better results (Table 5.5, Figure 5.8). There are multiple factors contributing to this. First, we note that Whitehall is a well-managed, simpler area as has been established in the previous chapter. Secondly, prob-

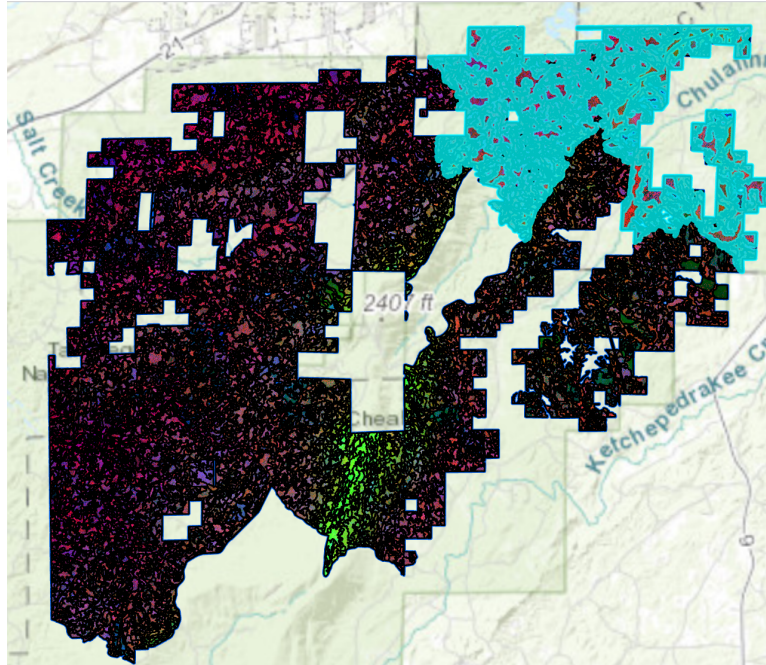


Figure 5.5: Nearly 310 stands created by the expert by merging microstands. Microstands merged over neighboring compartments within the study area.

lematic polygons such as roads were masked out before executing the algorithm. The roads themselves contribute highly to the way that the forest has historically been managed and thus how the stands were formed and separated. However, even through visual interpretation, we can see that important distinctions between neighboring stands were made well, with the only incorrect microstands being those that were not merged. For a smaller, simpler region like Whitehall, a simple post-processing step of eliminating smaller polygons, or even a quick selection and elimination step would easily turn this into a high quality stand map.

Our results over Whitehall indicate that in the case of simpler landscapes, with basic preprocessing (masking out roads) defining many of the stands, both of our approaches towards delineation work well.

Table 5.3: Evaluation metrics for stands created by the human-involved approach, where approximately 310 ‘real’ stands were formed across disjoint compartments in the larger Talladega region. The obtained results for every row were almost identical to the strategy where the user delineated disconnected components of stands. This can have multiple implications: 1) The user delineation strategy has little to no effect on the final delineations, as long as a certain amount of training samples are created. 2) As the initial microstand map used in both cases were the same, it plays a very big role in the final delineation. 3) The random forest algorithm does not fit the data well.

| Leaf Size | Probability Threshold | IoU | $RA_{or}\%$ | $RA_{os}\%$ | GS_{vol} | R_{vol}^2 | No. of Stands |
|-----------|-----------------------|-------------|-------------|-------------|------------|-------------|---------------|
| 5 | 0.5 | 0.20 | 57.7 | 50.3 | 0.67 | 0.26 | 1834 |
| 5 | 0.6 | 0.17 | 36.3 | 49.0 | 0.50 | 0.44 | 4854 |
| 5 | 0.7 | 0.14 | 29.1 | 51.9 | 0.59 | 0.51 | 8059 |
| 5 | expert selected | 0.52 | 49.6 | 53.2 | - | - | 301 |
| 1 | 0.5 | 0.19 | 42.6 | 49.1 | 0.61 | 0.39 | 3512 |
| 1 | 0.6 | 0.16 | 31.9 | 50.5 | 0.59 | 0.48 | 6509 |
| 1 | 0.7 | 0.13 | 27.9 | 52.6 | 0.59 | 0.52 | 9071 |
| 1 | expert selected | 0.53 | 49.2 | 53.1 | - | - | 317 |

Table 5.4: Evaluation metrics for stands created by the human-involved approach, for the sample area used in the previous chapter.

| Stand Type | IoU | $RA_{or}\%$ | $RA_{os}\%$ | GS_{vol} | R_{vol}^2 | No. of Stands |
|-------------------------|------|-------------|-------------|------------|-------------|---------------|
| Reference | - | - | - | 0.56 | 0.32 | 53 |
| Homogeneity approach | 0.27 | 0.31 | 0.36 | 0.55 | 0.35 | 51 |
| Human involved approach | 0.23 | 38.8 | 50.8 | 0.63 | 0.26 | 87 |

However, putting in slightly more effort by going through the human-involved route, the user can be more confident in the generated stand map.

The results over the Talladega National Forest indicate that the stand map that is immediately generated by the homogeneity approach is more appealing than the one generated by the human-involved method with greedier, low-confidence probability thresholds. However, maps created by the human-involved approach with higher confidence thresholds, while oversegmented, are easier to improve via post-processing or reiteration of the workflow. This is not the case with using just the homogeneity method, where the generated map contains larger polygons that are difficult to adjust (Figure 5.9). There is a clear

Table 5.5: Evaluation metrics for stands created by the human-involved approach, for the Whitehall area with masked out roads. Observed much higher alignment and results over this area as seen in 5.8.

| Stand Type | IoU | $RA_{or}\%$ | $RA_{os}\%$ | GS_{CHM} | R^2_{CHM} | No. of Stands |
|-------------------------|------|-------------|-------------|------------|-------------|---------------|
| Reference | - | - | - | 0.57 | 0.74 | 122 |
| Homogeneity approach | 0.39 | 58.1 | 55.2 | 0.55 | 0.82 | 111 |
| Human involved approach | 0.42 | 56.3 | 61.2 | 0.58 | 0.79 | 134 |

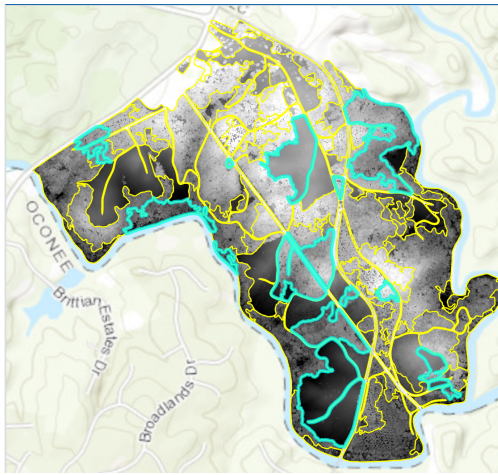


Figure 5.6: Generated Whitehall Map, showing selected areas

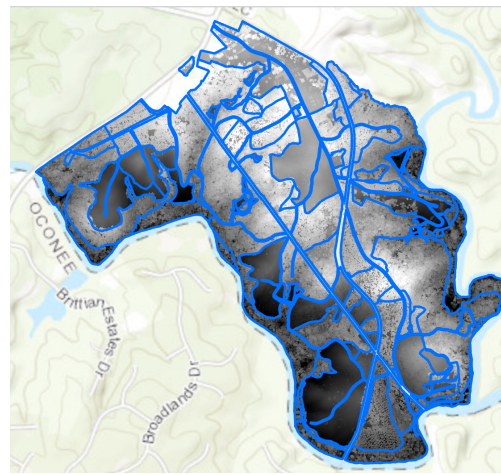


Figure 5.7: Reference Whitehall Map, roads masked out

Figure 5.8: Whitehall map derived by the human-involved approach, as presented in 5.5

trade-off between the amount of human effort needed versus the quality of the final map. However, the human-involved method does save effort when compared to the traditional way of delineating maps, with low loss of precision. The user can also adjust the confidence levels of the maps generated to a degree they feel comfortable with.

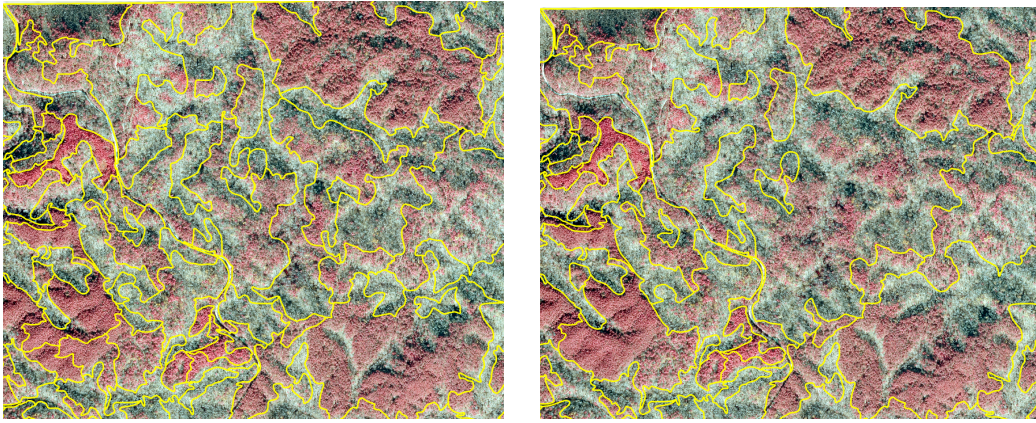


Figure 5.9: Talladega: High confidence threshold stands (left). Oversegmented, requiring post-processing or reiteration of the human-involved method. Requires effort but simpler to fix. (Right) Low confidence threshold. Undersegmented, difficult to fix once generated.

CHAPTER 6

CONCLUSION

This study aimed to automate the stand delineation process, a process which is frequently performed by forestry professionals. Stand delineation can be exhausting, and delineating larger areas can often take professionals multiple weeks. Research has only slowly begun to pick-up on this specific task with a focus on forest management planning. Some of the early research that was performed a decade ago does not hold up to the standards and expectations that we have from technology and AI today. Given the large scope of this problem, some of the modern works have now dedicated their attention to smaller subproblems, such as the idea of first establishing high quality microstands.

Our work sheds light on some of the issues that experts may have faced or overlooked when approaching this problem. We made effective use of high resolution optical imagery and LiDAR derived metrics with two strategies for automating the delineation process.

The first strategy was a quick and flexible way of creating stand maps, using the in-built mean shift segmentation tool in ArcGIS Pro and effective ways of calculating and merging microstands to maximize homogeneity while maintaining practically feasible stand sizes. We achieved varying degrees of success

which depended on the complexities of the landscapes involved. Issues such as the traditional unsupervised metrics favoring smaller stands were brought up. It was noted that while the generated stand maps did maximize homogeneity, the method was not well equipped to manage the user preferences or to understand implicit constraints that were not well represented by the LiDAR and aerial images.

A second strategy was thus presented which would both guide and be guided by the user along the way. The technique provides a simpler way for users to create candidate stand maps with minimal loss of precision. The candidate stand maps serve as training data to an underlying random forest model, which can then delineate the remaining stands itself. The model worked well on easier landscapes such as the Whitehall Forest, but it struggled to capture the complexities of the Talladega National Forest, even with a large number of data points. The model nevertheless was effective at merging some of the obvious stands. The process of merging and inference by the model for high confidence microstands could be done iteratively, resulting in an easier workflow for the end user.

There is great scope for improvement on these methodologies, with perhaps more complex AI models and improvements on the features used for training. As of now, there are no deep learning models that can handle delineation over such large areas while also being adaptive to the varying natures of forests around the world. Conversations with practicing foresters have lead to great excitement and a need for a solution to this problem. For researchers in the computer science/AI domain, the problem statement is rich with ideas that could be expanded upon and extended to other areas.

With that being said, however, when conducting experiments and research in this topic, we found that one of two things tended to be overlooked. First, there is an overreliance on existing methods and metrics that, while useful for a wide variety of geospatial and image analysis tasks, may not be suitable for stand delineation. A deep understanding of the underlying automation algorithms is necessary to

explain unwanted artifacts and adapt the methodologies accordingly. On the other end, experiments may be overly tailored to meet the requirements of a very specific study area with an abundance of resources, which may end up trivializing the problem. In order to create a generalized strategy for automating the stand delineation process, the methodology must be adaptable across varying landscapes with minimal data requirements. Forestry objectives must be well-defined and translatable to an algorithmic workflow. Thus, in order to come up with an effective solution to this task, collaboration between forestry and AI experts is imperative.

BIBLIOGRAPHY

- [1] US Department of Agriculture. *National Agricultural Imagery Program, Orthoimages*. <https://datagateway.nrcs.usda.gov/>.
- [2] Wei Chen et al. “Airborne LiDAR Remote Sensing for Individual Tree Forest Inventory Using Trunk Detection-Aided Mean Shift Clustering Techniques”. In: *Remote Sensing* 10 (July 2018), p. 1078. DOI: 10.3390/rs10071078.
- [3] D. Comaniciu and P. Meer. “Mean shift: a robust approach toward feature space analysis”. In: *IEEE Transactions on Pattern Analysis and Machine Intelligence* 24.5 (2002), pp. 603–619. DOI: 10.1109/34.1000236.
- [4] Clément Dechesne et al. “Semantic segmentation of forest stands of pure species combining airborne lidar data and very high resolution multispectral imagery”. In: *ISPRS Journal of Photogrammetry and Remote Sensing* 126 (2017). ISSN: 09242716. DOI: 10.1016/j.isprsjprs.2017.02.011.
- [5] Caner Demirpolat and Ugur Murat Lelogly. “Forest stand segmentation with multi-temporal Sentinel-2 imagery and superpixels”. In: *Journal of Applied Remote Sensing* 18 (Mar. 2024). DOI: <https://doi.org/10.1117/1.JRS.18.014530>.

- [6] Juan Carlos Niebles Fei-Fei Li. *Lecture 13: k-means and mean-shift clustering*. http://vision.stanford.edu/teaching/cs131_fall1617/lectures/lecture13_kmeans_mean_shift_cs131_2016.
- [7] Trimble Germany GmbH. *Trimble Documentation eCognition Developer 10.1 Reference Book*. 2021.
- [8] Xiong H. et al. “Forest stand delineation using airborne LiDAR and hyperspectral data.” In: *Silva Fennica vol. 58 no. 2 article id 23014* (2024).
- [9] Tin Kam Ho. “Random decision forests”. In: *Proceedings of 3rd international conference on document analysis and recognition*. Vol. 1. IEEE. 1995, pp. 278–282.
- [10] Stober J., K. Merry, and Bettinger P. “Analysis of fire frequency on the Talladega National Forest, USA, 1998-2018”. In: *International Journal of Wildland Fire*, 29, pp. 919-925 (2020).
- [11] Brian Johnson and Zhixiao Xie. “Unsupervised image segmentation evaluation and refinement using a multi-scale approach”. In: *ISPRS Journal of Photogrammetry and Remote Sensing* 66.4 (2011), pp. 473–483. ISSN: 0924-2716. DOI: <https://doi.org/10.1016/j.isprsjprs.2011.02.006>. URL: <https://www.sciencedirect.com/science/article/pii/S0924271611000293>.
- [12] Yinghai Ke, Lindi J. Quackenbush, and Jungho Im. “Synergistic use of QuickBird multispectral imagery and LIDAR data for object-based forest species classification”. In: *Remote Sensing of Environment* 114 (6 2010). ISSN: 00344257. DOI: 10.1016/j.rse.2010.01.002.
- [13] Potticary A. L. et al. “Spatiotemporal Variation in the Competitive Environment, With Implications for How Climate Change May Affect a Species With Parental Care.” In: *Ecology and Evolution* 13, no. 4: e9972. (2023).

- [14] USGS Landsat Missions. *Landsat Normalized Difference Vegetation Index*. <https://www.usgs.gov/landsat-missions/landsat-normalized-difference-vegetation-index>.
- [15] V.J. Leppänen et al. “AUTOMATIC DELINEATION OF FOREST STANDS FROM LIDAR DATA”. In: *GEOBIA, 2008—Pixels, Objects, Intelligence: GEOgraphic Object Based Image* (2008).
- [16] Ulas Yunus Ozkan et al. “Examining LiDAR – WorldView-3 data synergy to generate a detailed stand map in a mixed forest in the north-west of Turkey”. In: *Advances in Space Research* 65 (11 2020). ISSN: 18791948. DOI: 10.1016/j.asr.2020.02.020.
- [17] Timo Pukkala. “Correction to: Delineating forest stands from grid data”. In: *Forest Ecosystems* 7 (1 2020). DOI: 10.1186/s40663-020-00235-2.
- [18] Timo Pukkala. “Delineating forest stands from grid data”. In: *Forest Ecosystems* 7 (1 2020). ISSN: 21975620. DOI: 10.1186/s40663-020-00221-8.
- [19] Carter R.E. and Cobb G.C. “Woody species composition following a wildfire in the Dugger Mountain Wilderness, Talladega National Forest”. In: *Alabama Academy of Science*, 83(1): 1–7 (2012).
- [20] Jean-Romain Roussel, Tristan R.H. Goodbody, and Piotr Tompalski. <https://r-lidar.github.io/lidRbook/>.
- [21] Nuria Sanchez-Lopez, Luigi Boschetti, and Andrew T. Hudak. “Semi-automated delineation of stands in an even-age dominated forest: A LiDAR-GEOBIA two-stage evaluation strategy”. In: *Remote Sensing* 10 (10 2018). ISSN: 20724292. DOI: 10.3390/rs10101622.
- [22] Böck Sebastian, Immitzer Markus, and Clement Atzberger. “On the Objectivity of the Objective Function—Problems with Unsupervised Segmentation Evaluation Based on Global Score and a

- Possible Remedy”. In: *Remote Sensing* 9.8 (2017). ISSN: 2072-4292. DOI: 10.3390/rs9080769.
URL: <https://www.mdpi.com/2072-4292/9/8/769>.
- [23] Michael Snyder. *What is a Forest Stand (and Why do Foresters Seem so Stuck on Them)?* <https://northernwoodlands.org/articles/article/forest-stand>.
- [24] Yusen Sun et al. “A Comparison of Four Methods for Automatic Delineation of Tree Stands from Grids of LiDAR Metrics”. In: *Remote Sensing* 14 (24 2022). ISSN: 20724292. DOI: 10.3390/rs14246192.
- [25] Lee T et al. “The effects of nearby trees on the positional accuracy of GNSS receivers in a forest environment.” In: *PLoS ONE* 18(3): e0283090. (2023).
- [26] Pukkala T. et al. “A hybrid method for delineating homogeneous forest segments from LiDAR data in Catalonia (Spain)”. In: *European Journal of Remote Sensing*, 57(1) (2024).
- [27] Can Vatandaşlar et al. “Semi-Automatic Stand Delineation Based on Very-High-Resolution Orthophotographs and Topographic Features: A Case Study from a Structurally Complex Natural Forest in the Southern USA”. In: *Forests* 16 (Apr. 2025), p. 666. DOI: 10.3390/f16040666.